Targeting brain inflammation with bioconjugated nanoparticles

Anjali Hirani

Thesis submitted to the faculty of the Virginia Polytechnic Institute and State University
in partial fulfillment of the requirements for the degree of

Master of Science

In

Biomedical Engineering and Sciences

Yong Woo Lee, Committee Chair

Marion Ehrich

Aaron Goldstein

June 9, 2009

Blacksburg, VA

Keywords: Inflammation, Neurodegenerative disease, Nanoparticles

Targeting brain inflammation with bioconjugated nanoparticles

Anjali Hirani

Abstract

Brain inflammation has been implicated with the pathogenesis of neurodegenerative diseases. Activated microglia and endothelial cells induce production of reactive oxygen species (ROS) and overexpress pro-inflammatory mediators that perpetuate tissue damage. Current treatments are not effective against progressive stages of neurodegenerative diseases and more advanced therapies need to be developed. Recently, nanomaterials have been investigated for therapeutic applications. Nanoparticles can increase efficiency of drug delivery due to increased tissue distribution and the ability to modify surface chemistry to increase biocompatibility and incorporate targeting moieties.

In the present study, we established *in vitro* and *in vivo* brain inflammation models by administering lipopolysaccharide to mouse brain endothelial cells, microglia, macrophage cells and C57BL/6 male mice. Changes in mRNA expression of pro-inflammatory mediators were analyzed by real-time reverse transcriptase-polymerase chain reaction (RT-PCR). Tumor necrosis factor-α (TNF-α), interleukin-1β (IL-1β), interleukin-6 (IL-6), monocyte chemotactic protein-1 (MCP-1), E-selectin, and intercellular adhesion molecule-1 (ICAM-1) displayed significant overexpression when compared to the control. Additionally, folate receptor-α (FR-α) was also overexpressed, confirming that our model will function appropriately for specific targeting experiments.

Cellulose nanocrystals are rod-like particles, approximately 5 nm wide and 100-150 nm long. The surface area consists of extended hydroxyl groups and the structure is hydrophilic in nature. These characteristics make cellulose nanocrystals ideal for surface modification and ensuring long blood circulation half-life. Cell viability was determined using the MTT [3-(4,5-dimethylthiazol-2-yl)-2,5-diphenyltetrazolium bromide] conversion assay and a Lactate Dehydrogenase (LDH) Cytotoxicity Detection Kit. At each concentration of cellulose

nanocrystals (10, 25, 50 μg/mL), both assays showed the nanoparticles to be non-toxic. Binding/uptake experiments utilizing a fluorescence plate reader and fluorescence microscope showed no non-specific uptake of untargeted cellulose nanocrystals. In contrast, when conjugated to folic acid, cellulose nanocrystals were selectively incorporated to folate receptor-overexpressing cells.

These results indicate that both *in vitro* and *in vivo* brain inflammation models can be utilized to assess therapeutic efficacy of folate receptor-targeted bioconjugated nanoparticles.

Acknowledgments

I would like to express my gratitude and respect to my advisor, Dr. Yong Woo Lee for his guidance, encouragement and patience throughout my graduate studies. His scientific expertise, critical thinking and teaching ability are qualities that I aspire to achieve.

I want to acknowledge Dr. Marion Ehrich and Dr. Aaron Goldstein for serving on my committee. During the past several years, both of you have taken the time and effort to work with me individually. I will always remember and appreciate this.

I appreciate the help from our collaborators, Dr. Maren Roman and Shuping Dong, in the Department of Wood Science and Forest Products at Virginia Tech.

I especially want to thank my sister and parents for their continuous support, encouragement, and faith in me for pursuing my academic goals.

Finally, I would also like to thank my fellow lab members and close friends, Won Hee Lee and Paul Kim, who have become family to me. We have created a wonderful working environment together. Our graduate and department administrative staff, Tess Sentelle and Pam Stiff, will always have my thanks and good wishes for helping me.

Table of Contents

List of Figures

List of Abbreviations

AD: Alzheimer's disease
AP-1: activator protein-1
Aβ: amyloid β
BBB: blood-brain barrier
bEnd.3: Mouse brain microvascular endothelial cells
BV-2: Mouse microglia cells
C6 Glioma: Rat glioma cells
CNC: Cellulose nanocrystals
FA: Folic acid
FA-CNC-FITC: FITC-labeled, folic acid-conjugated cellulose nanocrystals
FITC: fluorescein-5'-isothiocyanate
FITC-CNC: FITC-labeled cellulose nanocrystals
FR-α: folate receptor-α
GAPDH: glyceraldehyde-3-phosphate dehydrogenase
HBMEC: Human brain microvascular endothelial cells
ICAM-1: intercellular adhesion molecule-1
IFN-γ: interferon-γ
IL-1β: interleukin-1β
IL-6: interleukin-6
KB: Human oral epithelial cells
LDH: Lactate dehydrogenase
LPS: Lipopolysaccharide
MCF-10A: Human breast epithelial cells
MCP-1: monocyte chemotactic protein-1
MDA-MB231: Human breast carcinoma cells
MDA-MB468: Human breast carcinoma cells
MTT: MTT [3-(4,5-dimethylthiazol-2-yl)-2,5-diphenyltetrazolium bromide] conversion assay
NF-κB: nuclear factor-κB
NSAIDs: non-steroidal anti-inflammatory drugs
PC3: Human prostate cancer cells
PD: Parkinson's disease
RAW264.7: Mouse macrophage cells
ROS: reactive oxygen species
RT-PCR: reverse transcriptase-polymerase chain reaction
TNF-α: Tumor necrosis factor-α

1. Introduction

1.1. Role of brain inflammation in the development of neurodegenerative disease

Inflammation is defensive reaction of the immune system to the presence of any pathogens. Exaggerated immune response triggers the activation of immunomodulatory cells, such as microglia and macrophage cells, and stimulates the release of pro-inflammatory mediators, such as cytokines and reactive oxygen species (ROS). Chronic inflammation is a significant component of neurodegenerative disease and irreversible damage attributed to neuroinflammatory mechanisms has been implicated in the pathophysiology of Alzheimer's disease (AD), Parkinson's disease (PD), and traumatic brain injury (Bone 2007).

Inflammation is a protective response naturally occurring in the vasculature in response to infection or irritation. The purpose of the inflammatory response is to remove the source of cell injury; however, chronic states of inflammation can lead to an overwhelming release of toxins and additional ROS. A chronic inflammatory state is indicated by increase in pro-inflammatory mediators, such as pro-inflammatory cytokines, chemokines, and adhesion molecules. The release of endothelial inflammatory mediators attracts blood leukocytes to injured tissue. Microglia and macrophages kill bacteria and foreign antigens; however, they also increase the degree of inflammation and cause tissue damage by releasing oxygen radicals (Vestweber 1992; Vestweber 2002).

Neuroinflammatory processes are significant in the pathogenesis of neurodegenerative diseases. Microglia activated in diseased systems exert similar destructive effects to microglia activated by invading microorganisms or endotoxins (Schwartz 2006). Activated microglia produce pro-inflammatory mediators that defend against pathogens; however, they have been implicated in brain damage in neurodegenerative diseases such as multiple sclerosis, AD, PD (Rock 2006).

Activated microglia produce pro-inflammatory mediators and reactive oxygen species which lead to transendothelial migration of immune cells across the blood-brain barrier. The

inflammatory response triggers astrocytes and endothelial cells resulting in a perpetuating cycle of inflammation and tissue damage (Mosley 2006).

The blood-brain barrier (BBB) is a highly selective barrier between blood and brain which regulates the entry of intravascular substances into the brain tissue (Rubin 1999). Brain microvascular endothelial cells are responsible in large part for the structure and function of the BBB. These cells form an uninterrupted capillary wall that provides the brain with a selective transport mechanism. Extracellular stimuli have been noted to trigger the brain microvascular endothelium to initiate several cascades of events leading to perturbations in the functional integrity of brain microvasculature and BBB leakage (Rubin 1999). Alterations of the brain microvasculature and disruption of the BBB are commonly found in patients with neurological disorders, such as AD, PD, and dementia (Staddon 1995; Rubin 1999; Toborek 2005).

It has been proposed that brain injury can be induced by external stimuli associated with oxidative stress (Kaur 1997). Oxidative stress can induce overexpression of pro-inflammatory mediators *via* redox-responsive transcription factor-mediated molecular signaling pathways. Expression of many inflammatory genes is up-regulated by increased oxidative stress through activation of transcription factors such as nuclear factor-κB (NF-κB) and activator protein-1 (AP-1) (Fahrig 2005). NF-κB and AP-1 are ubiquitously expressed, dimeric transcription factors that control cellular processes ranging from cell proliferation to cell death. Many neurodegenerative diseases are characterized by an inflammatory response and activation of NF-κB and AP-1. For example, amyloid β (Aβ) peptides are believed to contribute to pathogenesis in AD through pro-oxidative and pro-inflammatory mechanisms. Previous studies have shown that Aβ-induced oxidative stress in the brain can lead to an inflammatory cascade *via* secretion of interferon-γ (IFN-γ) and interleukin-1β (IL-1 β), as well as expression of CD40 in human brain microvascular endothelial cells (Suo 1998; de la Torre 2000). It was also demonstrated that Aβ increases the ability of monocytes/macrophages to transmigrate across the brain microvascular endothelial cell monolayer (Fiala 1998; Giri 2002). Additionally, oxidative stress and inflammation in the brain have been suggested to actively participate in the neurodegenerative process of PD (McGeer 2001; Schulz 2004). For example, degeneration of nigral dopaminergic neurons is observed in both an inflammation-mediated rat model and an *in*

vitro cell culture model of PD (Liu 2003). Evidence has suggested that treatment with antioxidant compounds or non-steroidal anti-inflammatory drugs (NSAIDs) may be associated with a lower risk of developing neurodegenerative diseases including AD and PD (Perry 1995; Moosmaan 2002; McGeer 2004). These findings provide compelling evidence that oxidative stress-mediated inflammatory responses in the brain may play a significant role in the pathogenesis of neurological disorders (Mechoulam 2002).

Endothelial cells line blood vessels and serve as an interface between blood and tissue. These cells are responsible for sensing changes in hemodynamics, oxygen pressure, and chemical signaling. They also are responsible for maintaining blood homeostasis by releasing mediators such as nitric oxide and regulating the activity of surface enzymes and surface proteins or adhesion molecules. Oxidative stress also causes many changes in endothelial cells including expression of adhesion molecules, induction of procoagulant state, cytokine production and neutrophil activation. These changes are responsible for leukocyte adhesion and platelet activation. Activation of endothelial cells by ROS initiate severe inflammatory processes (Black 2004; Li 2004).

In correlation to oxidative stress, excess amounts of oxygen radicals can induce changes in the structure and function of tissue lining. In molecular signaling pathways, inflammatory proteins or mediators are regulated at the transcription level by transcription factors. The promoter region of the inflammatory genes contains binding sites for certain transcription factors. In this case, oxidative stress is a critical stimulator in activating redox-regulated transcription factors. Activation of these transcription factors can initiate an inflammatory response.

Nuclear factor-κB (NF-κB) and activator protein-1 (AP-1) are part of a general regulation of a number of inflammatory gene expressions by cellular oxidative stress. NF-kB and AP-1 are ubiquitously expressed transcription factors that control processes ranging from cell survival and proliferation, to death. As an example, expression of the inflammatory cytokine TNF-α gene is induced by increased oxidative stress through activation of NF-κB. NF-κB remains in an inactive form bound to an inhibitory protein in the cytoplasm. ROS initiate the phosphorylation of IκB, leading to the subsequent degradation of IκB. This frees NF-κB, leading to its nuclear

translocation and regulation of gene transcription of pro-inflammatory mediators. Chronic inflammation also produces ROS and can result in a feedback loop that intensifies the damage in cells and tissues (Sarkara 2006; Taniyama 2003; Valko 2007).

Neurodegenerative diseases are associated with local inflammatory response. Pro-inflammatory mediators such as cytokines and ROS released from endothelial cells and microglia provide a link between inflammation and neurodegenerative process. These neurodegenerative diseases might benefit from anti-inflammatory treatment; targeting chronic inflammation and its mechanism of action would subsequently ameliorate damaging effects on healthy cells and tissues.

1.2. Development of novel biomaterials for targeting brain inflammation

Selective targeting of diseased cells offers the potential to administer therapies more effectively. Currently, many treatments are administered systemically, allowing the treatment to affect both healthy and diseased cells in the body. Targeted drug delivery increases therapeutic effects of drugs and minimizes side effects and toxicity (Zhang 2008). The goal of targeted drug delivery is to accumulate the drug selectively in the target organ or tissue and to maintain the concentration in non-target organs and tissues below a critical minimum, thus preventing unwanted side-effects (Couvreur 2006). Selective accumulation of the drug can be achieved in different ways: a) by direct application of the drug into the affected organ or tissue, b) through leaks in the vasculature at the affected site, a phenomenon called “enhanced permeability and retention” (passive targeting), c) through pH- or temperature-sensitive drug release (physical targeting), or d) through vector molecules with high specific affinity toward the affected zone (active targeting).

Various biomaterials such as polymer conjugates, micelles, nanoparticles, and liposomes are used to deliver therapeutic agents to inflamed or diseased tissues (Yoo 2001; Yoo 2004). Certain qualities make some biomaterials more attractive for use in drug delivery. Important characteristics include materials that are biodegradable or removable from the system without leaving residues. Biomaterials should be non-immunogenic or aggregate-forming so that

distribution is not hampered. Additionally, they should be hydrophilic to inhibit adsorption of proteins at particle surface (Zhang 2001).

Recently, nanotechnology has been investigated for a wide range of diagnostic and therapeutic applications. Nanoparticles confer multiple advantages for specific targeting. Physical characteristics of the base nanoparticle offers a wide array of possibilities such as control over optical and chemical properties. Particle size affects tissue distribution, including the ability to penetrate the BBB. By altering surface characterization with bioactive molecules and targeting agents, nanoparticles can be taken in the cell *via* endocytosis and *in vivo* biocompatibility can be increased (Rosenthal 2002). Utilizing these properties offered by size, enhanced delivery to brain cells can be achieved (Cernak 2004). This technology might offer more effective therapy for treating neurodegenerative diseases.

In the present study, there are two objectives in developing bioconjugated nanoparticles for targeting brain inflammation in neurodegenerative disease:

1. Establish *in vitro* and *in vivo* brain inflammation models.
2. Develop novel bioconjugated cellulose nanocrystals to target brain inflammation.

2. Establishment of *in vitro* and *in vivo* brain inflammation models

2.1 Introduction

In a healthy brain, there is a balance between pro-inflammatory and anti-inflammatory mediators. In neurological disorders, microglia are activated and produce high levels of inflammatory cytokines that trigger further inflammatory responses from other brain cells. Lipopolysaccharide (LPS) is the toxic portion of the outer membrane of Gram-negative bacteria. It contributes to the development of sepsis, a systemic inflammatory response defined by secretion of pro-inflammatory mediators. Similar to any inflammatory event, the ROS damage tissues, as well as activate transcription factors, such as NF-κB to regulate cytokine production. Peripheral injection of LPS induces production of inflammatory cytokines. Systemic sepsis causes infiltration of activated leukocytes into the brain which leads to brain injury across BBB *via* inflammatory damage during early process of transendothelial migration (Godbout 2005; Zhou 2007).

For our brain inflammation models, we utilized LPS to initiate the pro-inflammatory cascade similar to profiles documented for neurological disorders. In AD, PD, and multiple sclerosis, active microglia and peripheral macrophages have been reported to secrete a large amount of pro-inflammatory cytokines, such as IFN-γ, TNF-α, IL-1β, IL-6 and upregulate enzymes that produce ROS. LPS has been used to model the inflammatory response evident in these neurodegenerative diseases (Mosley 2006; Rock 2006). Utilizing LPS-modulated inflammation to model neurodegenerative diseases has previously been show in the literature, but is being established in our laboratory for future work on bioconjugated nanoparticles.

2.2 Materials and Methods

2.2.1 Cell cultures

Mouse brain microvascular endothelial cells (bEnd.3) were obtained from American Type Culture Collection (ATCC; Manassas, VA). bEnd.3 were cultured in Dulbecco's modified Eagle's medium (Mediatech) supplemented with 10% fetal bovine serum and 1% penicillin-streptomycin.

Mouse microglia cells (BV-2) were received from Dr. Robbins at Wake Forest University School of Medicine. These cells were cultured in Dulbecco's modified Eagle's medium (Mediatech) supplemented with 5% fetal bovine serum and 1% penicillin-streptomycin.

Mouse macrophage cells (RAW264.7) were obtained from ATCC. RAW264.7 were cultured in RPMI1640 medium (Mediatech) supplemented with 10% fetal bovine serum and 1% penicillin-streptomycin.

All cells were cultured at 37 °C with 5% CO_2 /95% air under a humidified atmosphere.

Cell cultures were treated with a single dose of 100 ng/ml LPS for 1, 2, 4, and 8 hours. After exposure time was complete, cells were isolated and total RNA was obtained.

2.2.2 Animals

C57BL/6 male mice were purchased from Harlan (Indianapolis, IN). Animals were housed at the animal facilities at Virginia Polytechnic Institute and State University. They were maintained under environmentally controlled conditions and subject to a 12 hour light/dark cycle with food and water *ad libitum*.

C57BL/6 mice were administered with a single intraperitoneal injection of either PBS (Control) or with 500 μg/kg of LPS in PBS for 1, 2, 4, and 8 hours. After exposure time was complete, whole brain was isolated and frozen until total RNA was isolated.

All experiments were performed with approval of Virginia Tech Institutional Animal Care and Use Committee.

2.2.3 Real-time reverse transcriptase-polymerase chain reaction (RT-PCR)

Total RNA from cell cultures was isolated using the RNeasy Mini Kit (Qiagen) according to the protocol of the manufacturer. Total RNA from mouse brains was isolated using Trizol reagent (Invitrogen) according to the protocol of the manufacturer. 1 μg of total RNA was reverse transcribed at 25 °C for 15 min, 42 °C for 45 min, and 99 °C for 5 min in 20 μl of 5 mM $MgCl_2$, 10 mM Tris-HCl, pH 9.0, 50 mM KCl, 0.1% Triton X-100, 1 mM dNTP, 1 unit/μl of recombinant RNasin ribonuclease inhibitor, 15 units/μg of AMV reverse transcriptase and 0.5 μg of random hexamers. Amplification of individual genes was performed on the Applied Biosystems 7300 Real-Time PCR System using TaqMan® Universal PCR Master Mix and a standard thermal cycler protocol (50 °C for 2 min before the first cycle, 95 °C for 15 sec, and 60 °C for 1 min, repeated 45 times). For specific probes and primers, TaqMan® Gene Expression Assay Reagents for mouse glyceraldehyde-3-phosphate dehydrogenase (GAPDH) (housekeeping gene), as well as mouse TNF-α, IL-1β, IL-6, MCP-1, E-selectin, and ICAM-1 were obtained from Applied Biosystems. The threshold cycle (C_T) was determined from each well using the Applied Biosystems Sequence Detection Software v1.2.3. C_T indicates the fractional cycle number at which the amount of amplified target gene reaches a fixed threshold. Relative quantification, or the change in gene expression from real-time quantitative PCR experiments between control and treatment groups, was calculated by the comparative C_T method (Livak 2001). Data was analyzed using equation $2^{-\Delta\Delta CT}$, where $\Delta\Delta C_T$ = [C_T of target gene - C_T of housekeeping gene] $_{\text{treated group}}$ - [C_T of target gene - C_T of housekeeping gene] $_{\text{control group}}$. Evaluation of $2^{-\Delta\Delta CT}$ gives the fold change in gene expression, which is normalized to a housekeeping gene (GAPDH) and relative to the control group.

2.2.4 Statistical Analysis

Quantitative data was obtained and analyzed using SigmaStat 3.5 (Systat Software, Inc., Point Richmond, CA). One-way ANOVA was used to compare mean responses among the treatments. For each endpoint, the treatment mean was compared using Bonferroni least significant difference procedure. Data is presented as means ± SD or SEM of at least three independent determinations, and statistical probability of $p < 0.05$ is considered significant.

2.3 Results and Discussion

As stated previously, LPS induces production of inflammatory cytokines and ROS similar to the pathogenesis of several neurodegenerative diseases. To establish our brain inflammation model, the effects of LPS on the expression of pro-inflammatory mediators was studied in mouse brain endothelial cells, microglial cells, macrophage cells and mouse brain. Expression levels of cytokines, chemokines and adhesion molecules were determined by quantitative real-time RT-PCR.

As shown in the Figure 1, mouse brain endothelial cells displayed a significant increase in several inflammatory mediators immediately after exposure to 100 ng/ml LPS. bEnd.3 cells showed an early response to IL-6 expression at 1 hour exposure that continued to increase 15-fold at 4 hour exposure, before attenuating response at 8 hours. MCP-1 expression increased steadily throughout time exposure until it reached almost 100-fold overexpression. E-selectin reached 25-fold increased expression at 2 hour exposure, before it attenuated. ICAM-1 showed a significant response after 2 hour exposure. It peaked at 10-fold response during 4 hour exposure.

Mouse microglial cells (Figure 2) also displayed a significant increase in inflammatory mediators immediately after exposure to 100 ng/ml LPS. IL-6 was overexpressed immediately after LPS exposure. It displayed a 1000-fold increase at 4 hour exposure, after which IL-6 response began to decrease. TNF-α response in BV-2 cells peaked after 1 hour exposure and slowly declined. MCP-1 expression increased steadily throughout time exposure.

Mouse macrophage cells (Figure 3) exhibited increased expression in TNF-α, IL-1β, and IL-6 after exposure to 100 ng/ml LPS. TNF-α reached a 35-fold induction that remained

consistent until 8 hours of exposure. IL-1β and IL-6 displayed expression levels that increased constantly and significantly over time, reaching 2,500-fold induction.

C57BL/6 mice were administered with 500 μg/kg of LPS. When compared to the control, TNF-α, IL-1β, IL-6, MCP-1, E-selectin, and ICAM-1 in whole brain extracted from mice displayed significant increases in expression throughout total time exposure (Figure 4).

There was a significant change in expression of pro-inflammatory mediators in the cell lines and mice tested. These results show a gene expression profile indicating an exaggerated neuroinflammatory response when lipopolysaccharide is administered to brain endothelial and immune cells. These pro-inflammatory mediators have been reported to overexpress in neurodegenerative disorders. Therefore, these results demonstrate that we have established in vitro and in vivo brain inflammation models that can be utilized for developing and testing therapeutic efficacy of bioconjugated nanoparticles.

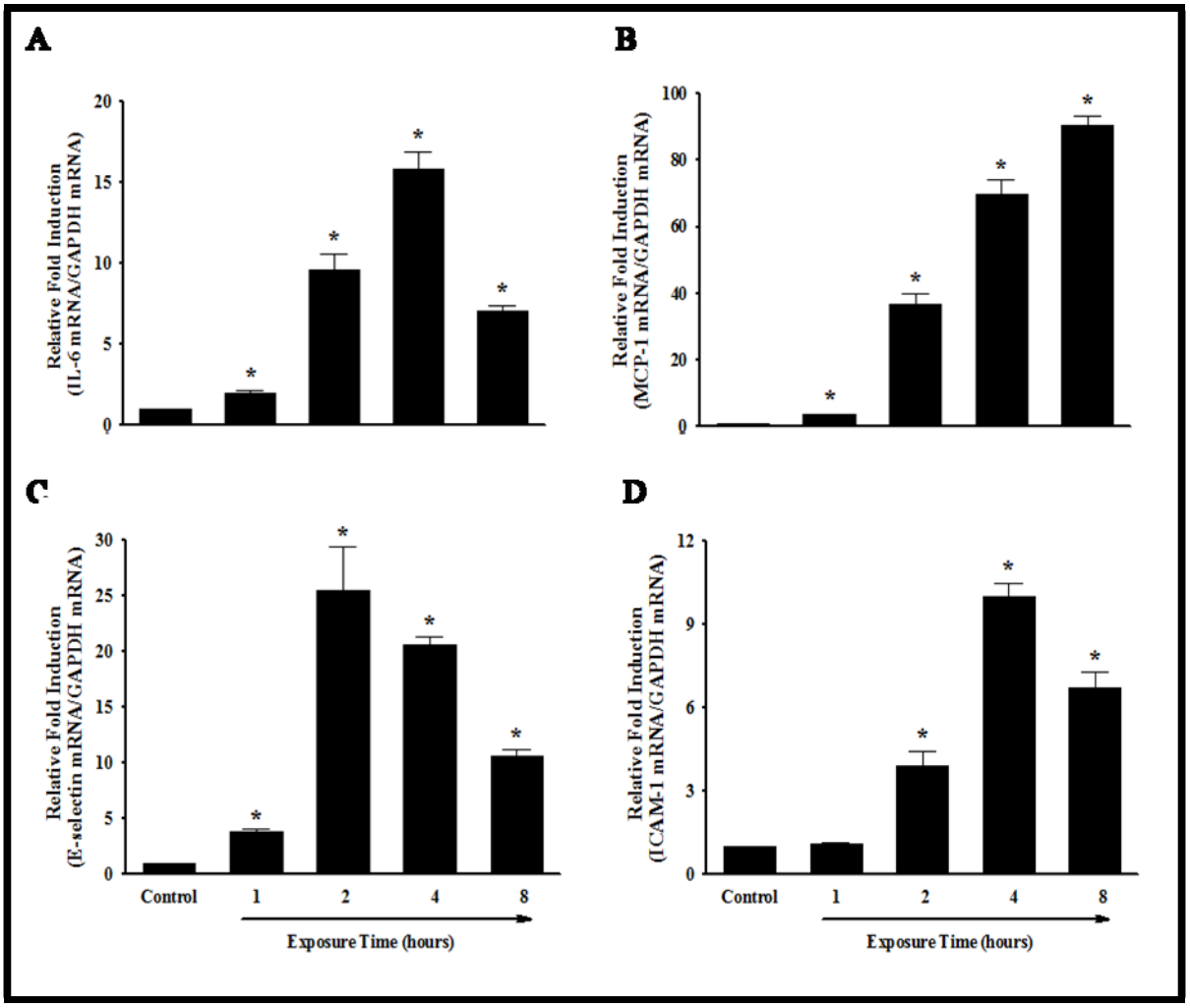

Figure 1: Effects of LPS on the expression of inflammatory mediators in mouse brain endothelial cells (bEnd.3). bEnd.3 cells were treated with 100 ng/ml LPS for 1, 2, 4, and 8 hours. Expression levels of pro-inflammatory mediators, IL-6 (A), MCP-1 (B), E-selectin (C), and ICAM-1 (D), were determined by quantitative real-time RT-PCR as described in Materials and Methods. Data are ±SEM of 4 determinations. *Statistically significant compared with control group ($p < 0.05$).

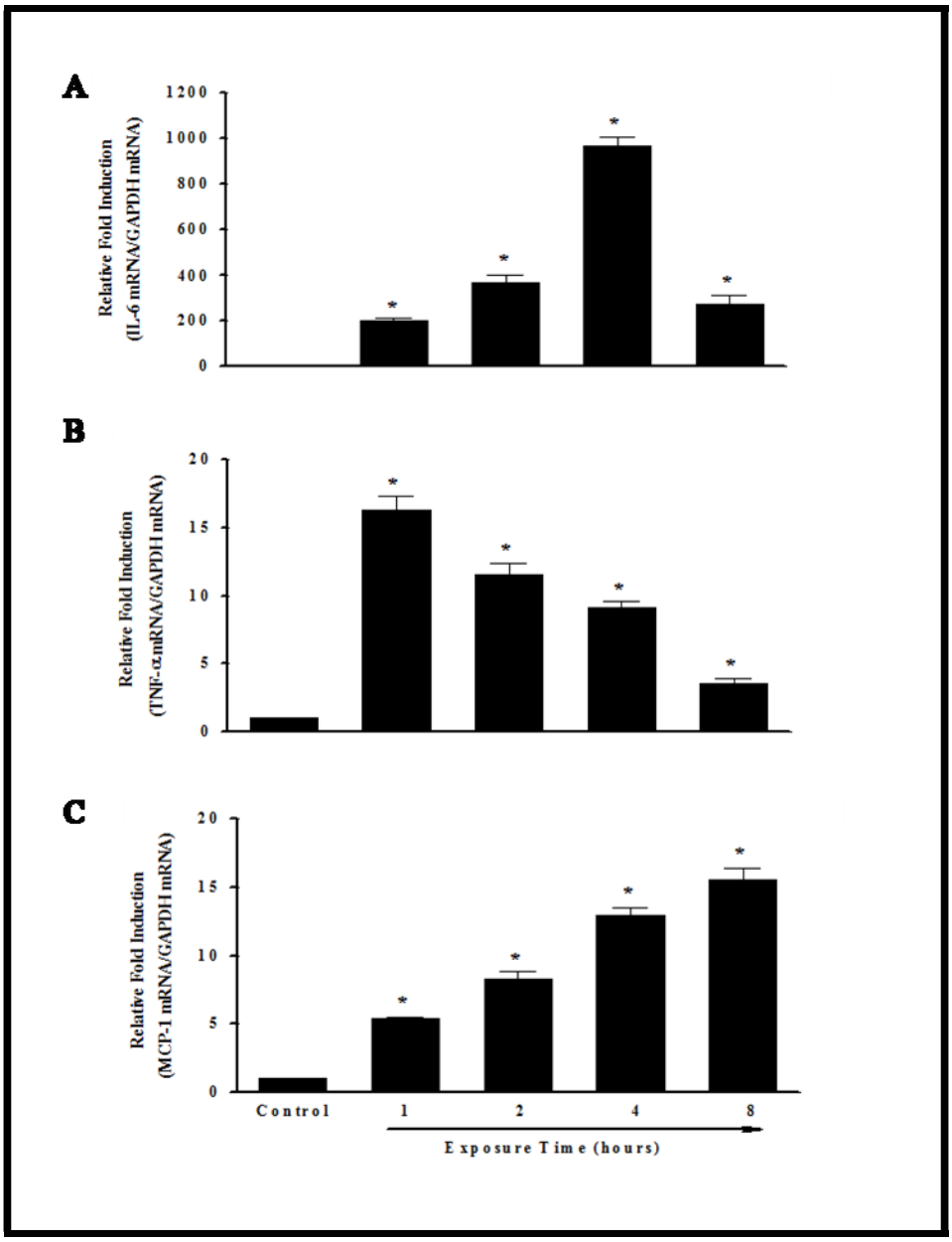

Figure 2: Effects of LPS on the expression of inflammatory mediators in mouse microglial cells (BV-2). BV-2 cells were treated with 100 ng/ml LPS for 1, 2, 4, and 8 hours. Expression levels of pro-inflammatory mediators, IL-6 (A), TNF-α (B), and MCP-1 (C) were determined by quantitative real-time RT-PCR as described in Materials and Methods. Data are ±SEM of 4 determinations. *Statistically significant compared with control group ($p < 0.05$).

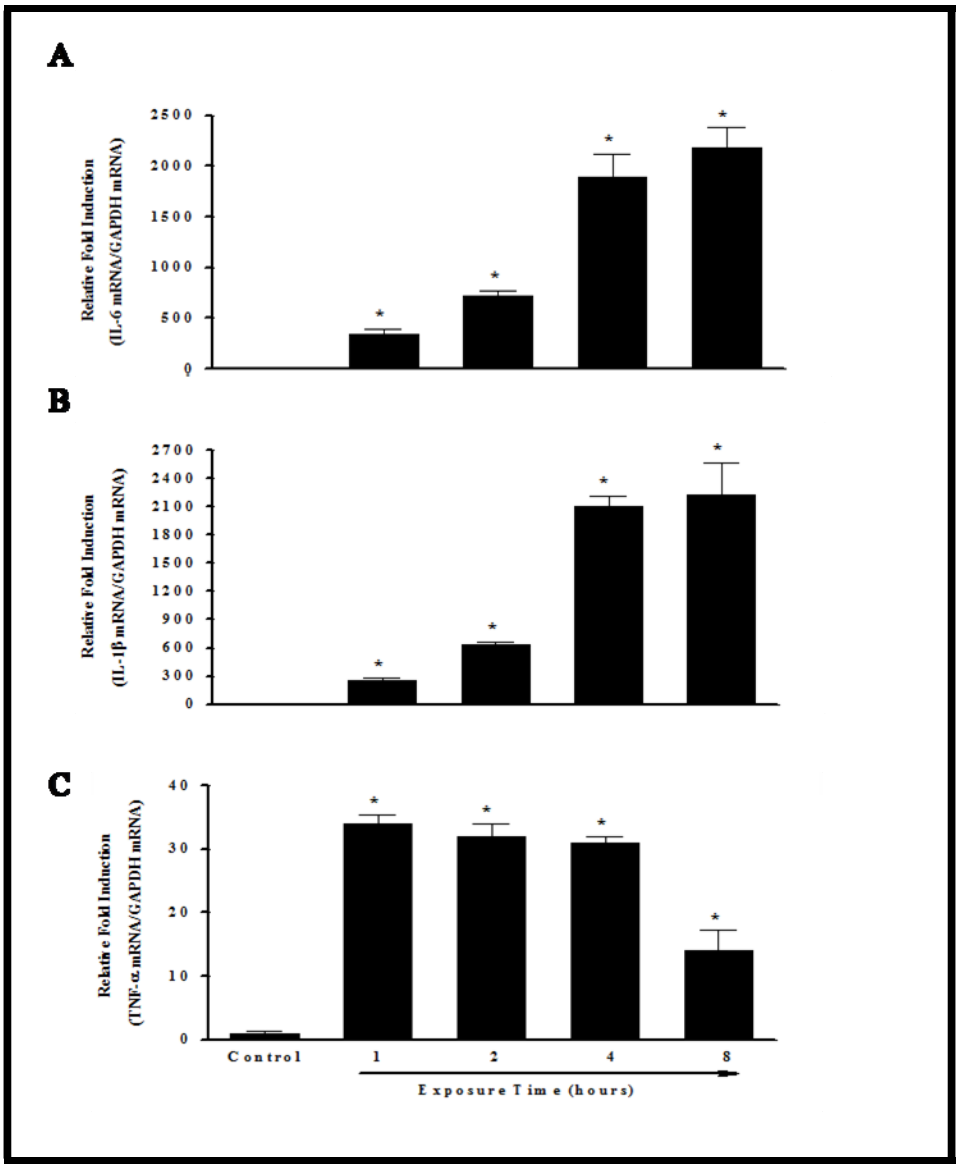

Figure 3: Effects of LPS on the expression of inflammatory mediators in mouse macrophages (RAW 264.7). RAW264.7 cells were treated with 100 ng/ml LPS for 1, 2, 4, and 8 hours. Expression levels of pro-inflammatory mediators, IL-6 (A), IL-1β (B), and TNF-α (C) were determined by quantitative real-time RT-PCR as described in Materials and Methods. Data are ±SEM of 4 determinations. *Statistically significant compared with control group ($p < 0.05$).

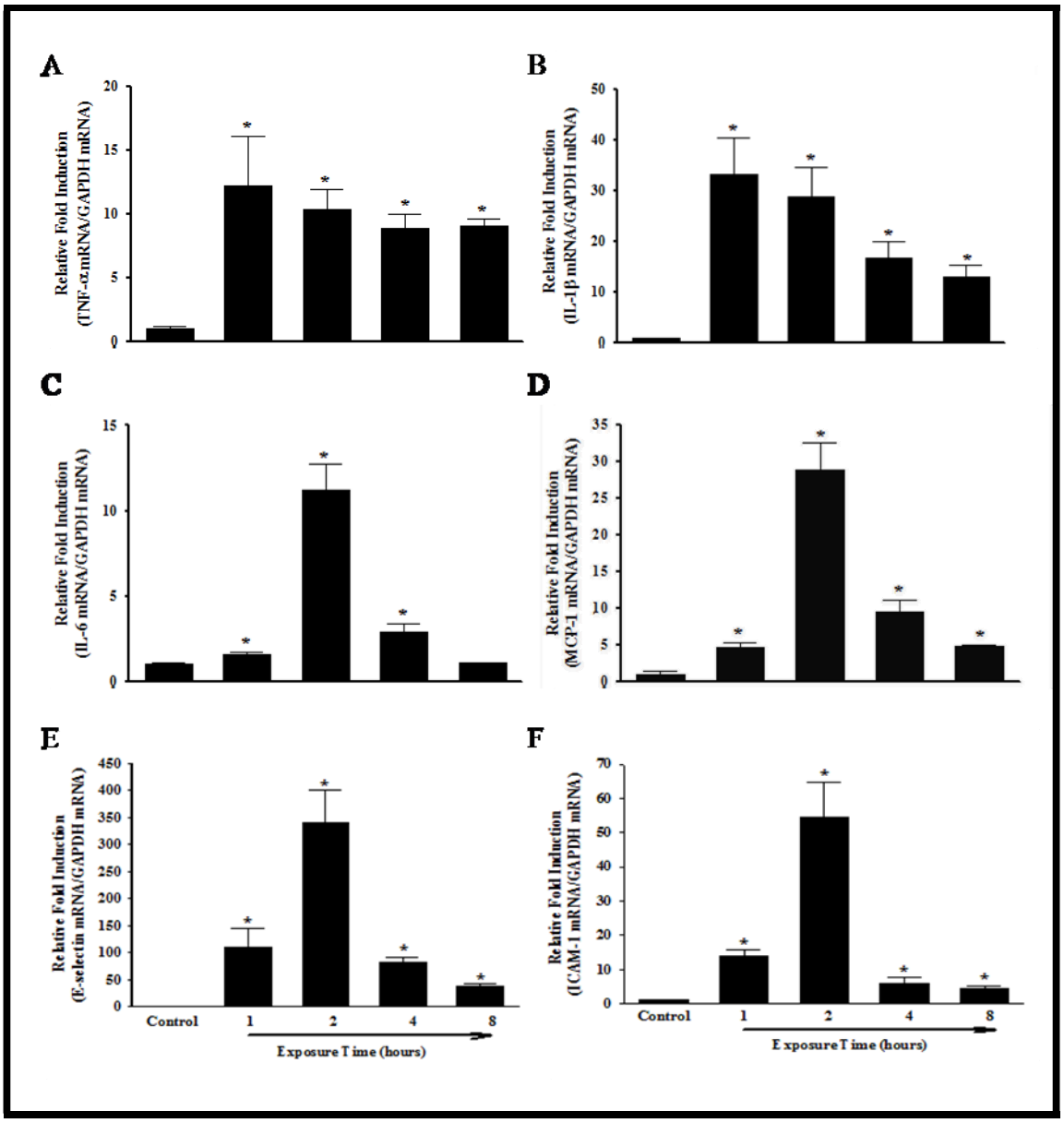

Figure 4: Effects of LPS on the expression of inflammatory mediators in mouse brain. Mice were treated with 500 μg/kg LPS for 1, 2, 4, and 8 hours. Expression levels of pro-inflammatory mediators, TNF-α (A), IL-1β (B), IL-6 (C), MCP-1 (D), E-selectin (E), and ICAM-1 (F) in whole brain extracts were determined by quantitative real-time RT-PCR as described in Materials and Methods. Data are ±SEM of 4 determinations. *Statistically significant compared with control group ($p < 0.05$).

3. Development of bioconjugated nanoparticles for targeting brain inflammation

3.1 Introduction

Targeted drug delivery increases effectivity of drug and minimizes side effects and toxicity (Zhang 2008). Various biomaterials such as polymer conjugates, micelles, nanoparticles, and liposomes are used to deliver therapeutic agents to inflamed or diseased tissues (Yoo 2001; Yoo 2004). Several factors can make certain biomaterials more attractive for use in drug delivery. The biomaterial should be degradable or removable from the system without leaving residues. It should not aggregate, otherwise distribution is hampered and it will be cleared from the system rapidly. Additionally, biomaterials that are hydrophilic inhibit adsorption of opsonin proteins at particle surface and prevent early clearance *via* phagocytes (Zhang 2001).

Cellulose nanocrystals are an ideal candidate as nanoscale drug carriers in targeted drug delivery applications. Cellulose nanocrystals are rod-like particles of cellulose microfibrils, prepared by acidic breakdown of cellulose fibers (Roman 2005). Cellulose nanocrystals have been used extensively as a model to study colloidal liquid crystalline phases (Marchessault 1959; Revol 1992; Revol 1994; Araki 1998; Dong 1998; Araki 2000). More recently, cellulose nanocrystals have gained attention as a biomaterial on the nanoscale due to their large surface area and high strength and stiffness (Favier 1995; Helbert 1996; Chazeau 1999; Grunert 2002). The potential use of cellulose nanocrystals as a targeted drug delivery system, however, has not yet been explored.

Cellulose is a linear homopolysaccharide of β-D-glucopyranose units connected through (1→4)-glycosidic bonds (Figure 5). The surface area of cellulose nanocrystals consists of extended hydroxyl groups; thus, the structure is highly hydrophilic. Due to the hydrophilic nature, cellulose nanocrystals exhibit low protein adsorption (Dumitriu 2002), ensuring a long blood circulation half-life and delaying initial clearance from the blood stream. Cellulose is

nontoxic and biocompatible (Sinha 1984; Holland 1997), and it does not trigger an inflammatory response.

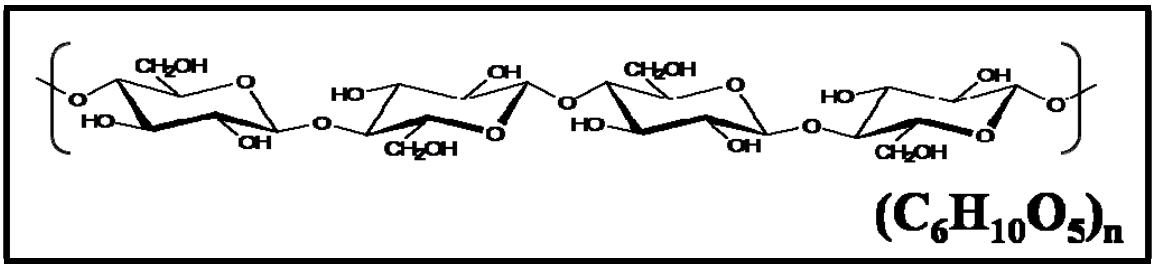

Figure 5: Chemical structure of cellulose.

Cellulose nanocrystals have a size range between 50 and 200 nm with the majority of the rod-like particles between 100 and 150 nm long. This size range is expected to be too large for removal from the blood stream by the renal system (i.e. the kidneys) but still small enough that the rate of clearance from the blood stream by the mononuclear phagocytic system (MPS) is delayed (Owens 2006). Being entirely composed of polysaccharide molecules, cellulose nanocrystals are highly hydrophilic in nature. A hydrophilic surface has been shown to impede adsorption of opsonin proteins, a critical step before phagocytosis during removal of nanoparticles from the blood stream (Lemarchand 2004). Thus, cellulose nanocrystals are expected to have an inherent prolonged blood circulation half-life as compared to hydrophobic particles. Cellulose can be degraded by reactive oxygen and nitrogen species, such as those used by phagocytes to break down the phagocytosed material (Carlsson 2005). Cellulose nanocrystals are therefore expected not to accumulate permanently in the MPS organs (e.g. liver and spleen). The surface chemistry of cellulose nanocrystals is governed by hydroxyl groups, which can be easily converted into other functional groups for covalent and non-covalent binding of targeting and/or drug moieties to the surface of the nanoparticles. By altering surface characterization, we can increase active targeting and *in vivo* biocompatibility.

3.2 Materials and Methods

3.2.1 Preparation of cellulose nanocrystals

Cellulose nanocrystals were prepared in Dr. Roman's laboratory in the Department of Wood Science and Forest Products at Virginia Tech by sulfuric acid hydrolysis of dissolving-grade softwood sulfite pulp. Lapsheets of the pulp (Temalfa 93A-A) were cut into small pieces of 1 cm by 1 cm and milled in a Wiley mill (Thomas Wiley Mini-Mill) to pass a 60 mesh screen. The milled pulp was hydrolyzed under stirring with 64 wt % sulfuric acid (10 ml/g cellulose) at 45 °C for 60 min. The hydrolysis was stopped by diluting the reaction mixture 10-fold with deionized water (Millipore Direct-Q 5, 18.2 MΩ·cm). The nanocrystals were collected and washed once with deionized water by centrifugation for 10 min at 25 °C and 4,550 × g (Thermo IEC Centra- GP8R) and then dialyzed (Spectra/Por 4 dialysis tubing) against deionized water until the pH of fresh dialysis medium stayed constant over time. The nanocrystal suspension was sonicated (Sonics & Materials Model VC-505) for 10 min at 200 W under ice-bath cooling and filtered through a 0.45 μm polyvinylidene fluoride (PVDF) syringe filter (Millipore) to remove any aggregates present.

3.2.2 FITC labeling of cellulose nanocrystals

Cellulose nanocrystals were labeled with fluorescein-5'-isothiocyanate (FITC) in Dr. Roman's laboratory. The FITC-labeling was a three-step reaction (Figure 6) (Dong 2007). First, the surface of the nanocrystals was layered with epoxy functional groups *via* reaction with epichlorohydrin (6 mmol/g cellulose) in 1 M sodium hydroxide (132 ml/g cellulose) (Porath 1970). After 2 h at 60 °C, the reaction mixture was dialyzed (Spectra/Por 4 dialysis tubing) against deionized water (Millipore Direct-Q 5, 18.2 MΩ·cm) until the pH was below 12. Next, the epoxy ring was opened with ammonium hydroxide to introduce primary amino groups. After adjusting the pH to 12 with 50% (w/v) sodium hydroxide, ammonium hydroxide (29.4%, 5 ml/g cellulose) was added and the reaction mixture was heated to 60 °C for 2 h. The reaction mixture was dialyzed until the pH was 7. Finally, the primary amino group was reacted with the isothiocyanate group of FITC to form a thiourea. FITC (0.32 mmol/g cellulose) was added to the

aminated nanocrystals in 50 mM sodium borate buffer solution (50 ml/g cellulose), containing ethylene glycol tetraacetic acid (5 mM), sodium chloride (0.15 M), and sucrose (0.3 M) (Swoboda 1985). The reaction mixture was stirred overnight in the dark and then dialyzed for 5 days. The suspension was sonicated (10 min, 200 W, ice bath cooling), centrifuged (10 min, 4,550 × g, 25 °C), and filtered through a syringe filter (0.45 μm) to remove any aggregates. The final suspension (0.5 wt %) had a pH of 6.

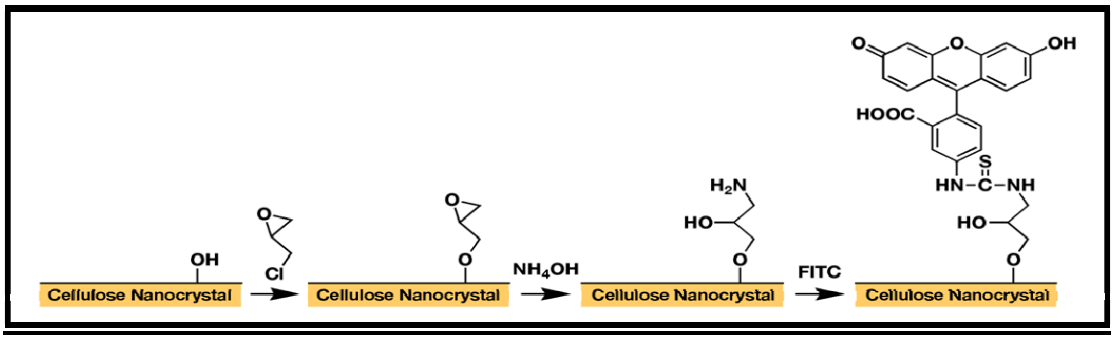

Figure 6: Schematic representation of conjugation of cellulose nanocrystals with FITC (FITC-CNC).

3.2.3 Folic acid conjugation of cellulose nanocrystals

Folic acid conjugation to FITC-labeled cellulose nanocrystals was performed in Dr. Roman's laboratory. Cellulose nanocrystals (CNCs) were labeled with fluorescein isothiocyanate (FITC) as illustrated in Figure 6 and folic acid was introduced and bound to the FITC-labeled cellulose nanocrystals as shown in Figure 7.

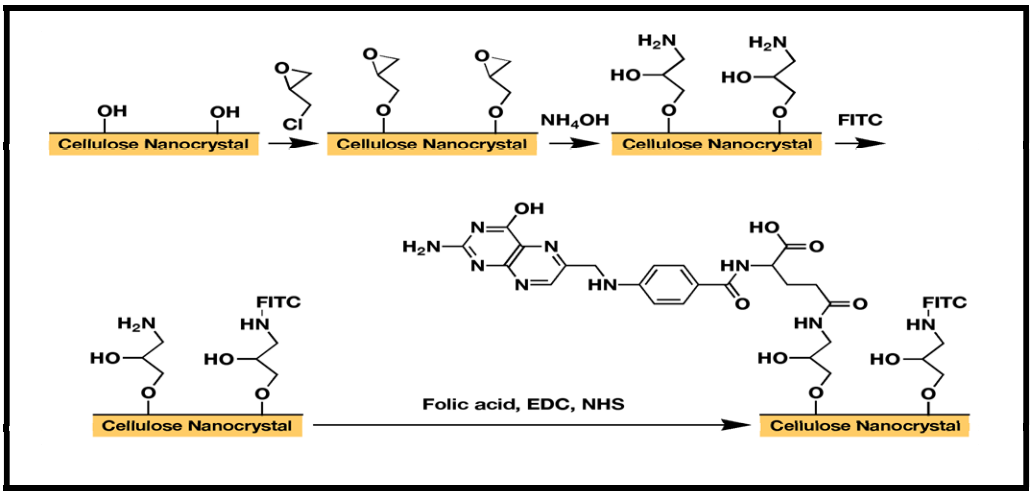

Figure 7: Schematic representation of conjugation of cellulose nanocrystals with FITC and Folic Acid (FA-CNC-FITC).

3.2.4 Cell cultures and animals

Human brain microvascular endothelial cells (HBMEC) were received from Dr. Toborek at the University of Kentucky Medical Center. These cells were originally isolated and purified as previously described (Stins 1997). HBMEC were cultured in RPMI1640 medium (Mediatech) supplemented with 10% fetal bovine serum, 10% NuSerum, endothelial cell growth supplement (30 μg/ml), heparin (15 U/ml), L-glutamine (2 mM), sodium pyruvate (2 mM), nonessential amino acids, vitamins, and penicillin-streptomycin.

Mouse brain microvascular endothelial cells (bEnd.3) were obtained from American Type Culture Collection (ATCC; Manassas, VA). bEnd.3 were cultured in Dulbecco's modified Eagle's medium (Mediatech) supplemented with 10% fetal bovine serum and 1% penicillin-streptomycin.

Primary rat astrocytes were isolated as previously described in Parran (2005). Astrocytes were cultured in Minimal Essential Medium supplemented with 10% horse serum.

Rat glioma cells (C6 glioma) were obtained from ATCC and were cultured in Dulbecco's modified Eagle's medium (Mediatech) supplemented with 10% fetal bovine serum and 1% penicillin-streptomycin.

Mouse microglia cells (BV-2) were received from Dr. Robbins at Wake Forest University School of Medicine. These cells were cultured in Dulbecco's modified Eagle's medium (Mediatech) supplemented with 5% fetal bovine serum and 1% penicillin-streptomycin.

Mouse macrophage cells (RAW264.7) were obtained from ATCC. RAW264.7 were cultured in RPMI1640 medium (Mediatech) supplemented with 10% fetal bovine serum and 1% penicillin-streptomycin.

Human breast epithelial cells (MCF 10A) were obtained from ATCC and were cultured in 1:1 Ham's F12 medium and Dulbecco's modified Eagle's medium (Mediatech) supplemented with 10% horse serum, epidermal growth factor (20 ng/ml), cholera toxin (100 ng/ml), insulin (0.01 mg/ml), hydrocortisone (500 ng/ml), and penicillin-streptomycin.

Human breast carcinoma cells (MDA-MB-468) were obtained from ATCC and maintained in Dulbecco's modified Eagle's medium (Mediatech) supplemented with 10% fetal bovine serum and 1% penicillin-streptomycin.

Human breast carcinoma cells (MDA-MB-231) were obtained from ATCC and maintained in Leibovitz's L-15 Medium (Mediatech) supplemented with 10% fetal bovine serum and 1% penicillin-streptomycin.

Human oral epithelial cells (KB) were obtained from ATCC and maintained in Minimal Essential Medium (Mediatech) supplemented with 10% fetal bovine serum, 1% penicillin-streptomycin, and L-glutamine (2 mM), sodium pyruvate (2 mM), nonessential amino acids.

Human prostate cancer cells (PC3) were obtained from ATCC and maintained in RPMI1640 medium (Mediatech) supplemented with 10% fetal bovine serum and 1% penicillin-streptomycin.

All cells were cultured at 37 °C with 5% CO_2 /95% air under a humidified atmosphere.

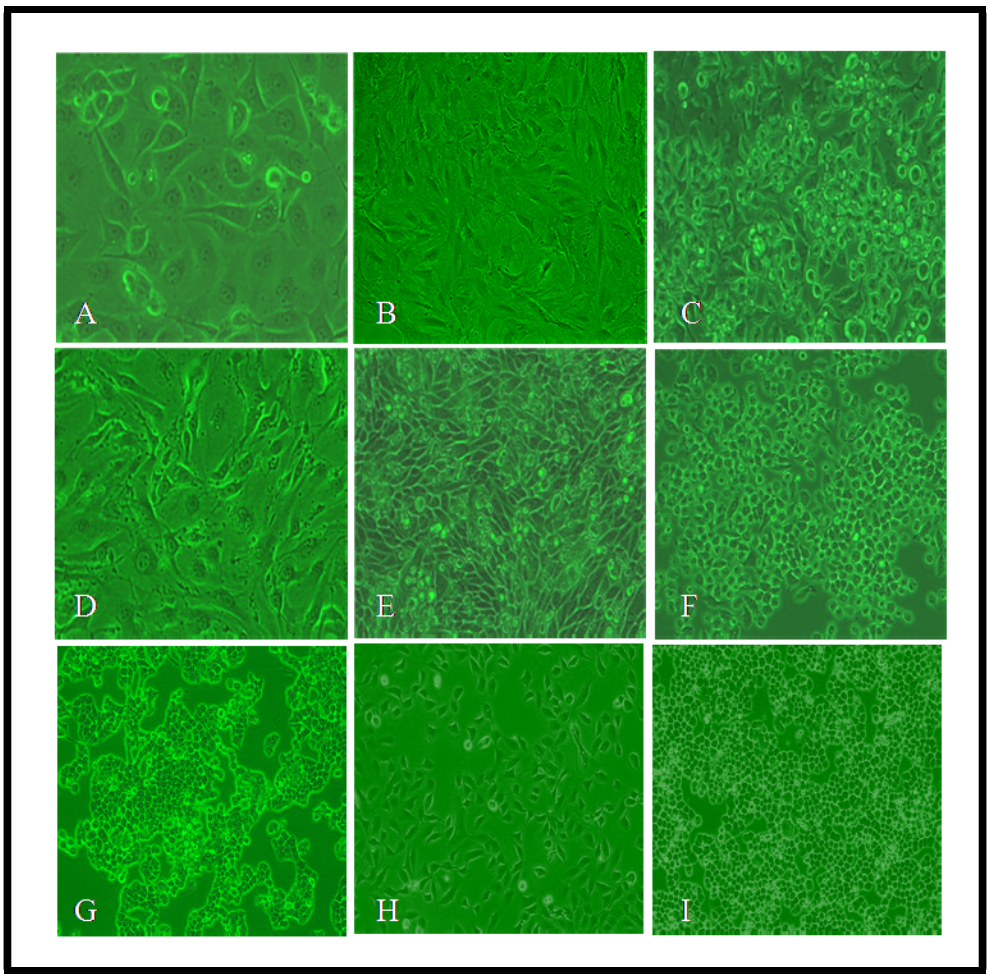

Figure 8: Micrographs of some cells used in the present study. Human brain microvascular endothelial cells (HBMEC) (A), Rat primary astrocytes (B), Mouse microglial cells (BV-2) (C), Mouse brain microvascular endothelial cells (bEnd.3) (D), Rat C6 Glioma Cells (E), Mouse macrophage cells (RAW264.7) (F), Human tumor oral epithelial cells (KB) (G), Human breast epithelial cells (MCF 10A) (H), Human breast carcinoma cells (MDA-MB-468) (I).

C57BL/6 male mice were purchased from Harlan (Indianapolis, IN). Animals were housed at the animal facilities at Virginia Polytechnic Institute and State University. They were maintained under environmentally controlled conditions and subject to a 12 hour light/dark cycle with food and water *ad libitum*. All experiments were performed with approval of Virginia Tech Institutional Animal Care and Use Committee.

3.2.5 Cell viability/cytotoxicity assay

Cell viability was determined using the MTT [3-(4,5-dimethylthiazol-2-yl)-2,5-diphenyltetrazolium bromide] conversion assay. It is a colorimetric assay which measures the metabolic activity of viable cells. The tetrazolium salt MTT is reduced to a colored water-insoluble formazan salt by mitochondria in active cells. All cell types were cultured in 48-well plates and treated with increasing concentrations of cellulose nanocrystals (0, 10, 25, and 50 μg/ml). After incubating 48 hours at 37 °C, treated cells were rinsed two times with phosphate-buffered saline (PBS) and incubated with MTT solution (0.5 mg/mL in basal medium) for 4 h at 37°C. The insoluble colored formazan salts were dissolved in dimethyl sulfoxide (DMSO) and the absorbance was assessed at 570 nm for each well. Data are shown in MTT conversion as a percentage of the control; cell death would be shown by a significant decrease in values below 100%.

Additionally, cytotoxicity was assessed using an LDH Cytotoxicity Detection Kit (Roche Applied Science). This assay measures the release of cytoplasmic enzyme lactate dehydrogenase (LDH) by damaged cells. Cells cultured in 48-well plates were treated with increasing concentrations of cellulose nanocrystals (0, 10, 25, and 50 μg/ml). After 48 hours of treatment, culture supernatant was collected and incubated with reaction mixture. The LDH-catalyzed conversion results in the reduction of the tetrazolium salt to formazan, which can be read at absorbance 490 nm. These data are measured in LDH activity as a percentage of the control. Any significant increase in LDH levels would indicate cellular disruption or death due to the treatment.

3.2.6 Cellular binding/uptake assay

For cellular binding/uptake studies, cells were incubated with 50 μg/mL of FITC-labeled cellulose nanocrystals for 1, 2, 4, and 8 hours. The cells were washed three times with PBS to remove any cellulose nanocrystals not taken up. The fluorescence intensity was determined with a fluorescence microplate reader (Molecular Devices SpectraMax M2e) at an excitation and emission wavelength of 485 and 530 nm, respectively.

Additionally, cellular binding/uptake was imaged using fluorescence microscopy. 1 mL of cells was seeded onto 4-well chamber slides (Lab-Tek) and incubated for 24 – 48 hours. Cells were washed with HBSS and fresh basal folate-free RPMI 1640 was added to the wells. Cells were treated with 100 μL FITC-labeled cellulose nanocrystals (FITC-CNC) or 100 μl FITC-labeled, folic acid-conjugated cellulose nanocrystals (FA-CNC-FITC) into each chamber and incubated for 4 hours at 37 ºC. An additional well was treated with 100 μL FITC-labeled, folic acid-conjugated cellulose nanocrystals (FA-CNC-FITC) in the presence of 1 mM free folic acid (FA). The excess free folic acid should block tumor folate receptors, preventing binding of the conjugated nanoparticles and demonstrate the binding specificity of our targeted particles.

3.2.7 Real-time RT-PCR

Total RNA from cell cultures was isolated using the RNeasy Mini Kit (Qiagen) according to the protocol of the manufacturer. Total RNA from mouse brains was isolated using Trizol reagent (Invitrogen) according to the protocol of the manufacturer. 1 μg of total RNA was reverse transcribed at 25 °C for 15 min, 42 °C for 45 min, and 99 °C for 5 min in 20 μl of 5 mM $MgCl_2$, 10 mM Tris-HCl, pH 9.0, 50 mM KCl, 0.1% Triton X-100, 1 mM dNTP, 1 unit/μL of recombinant RNasin ribonuclease inhibitor, 15 units/μg of AMV reverse transcriptase and 0.5 μg of random hexamers. Amplification of individual genes was performed on the Applied Biosystems 7300 Real-Time PCR System using TaqMan® Universal PCR Master Mix and a standard thermal cycler protocol (50 °C for 2 min before the first cycle, 95 °C for 15 sec, and 60 °C for 1 min, repeated 45 times). For specific probes and primers, TaqMan® Gene Expression Assay Reagents for mouse glyceraldehyde-3-phosphate dehydrogenase (GAPDH) (housekeeping gene) and FR-α were obtained from Applied Biosystems. The threshold cycle (C_T) was determined from each well using the Applied Biosystems Sequence Detection Software v1.2.3. C_T indicates the fractional cycle number at which the amount of amplified target gene reaches a fixed threshold. Relative quantification, or the change in gene expression from real-time quantitative PCR experiments between control and treatment groups, was calculated by the comparative C_T method (Livak 2001). Data was analyzed using equation $2^{-\Delta\Delta CT}$, where $\Delta\Delta C_T$ =

[C_T of target gene - C_T of housekeeping gene] $_{\text{treated group}}$ - [C_T of target gene - C_T of housekeeping gene] $_{\text{control group}}$. Evaluation of $2^{-\Delta\Delta CT}$ gives the fold change in gene expression, which is normalized to a housekeeping gene (GAPDH) and relative to the control group.

3.2.8 Statistical Analysis

Quantitative data was obtained and analyzed using SigmaStat 3.5 (Systat Software, Inc., Point Richmond, CA). One-way ANOVA was used to compare mean responses among the treatments. For each endpoint, the treatment mean was compared using Bonferroni least significant difference procedure. Data is presented as means ± SD or SEM of at least three independent determinations, and statistical probability of $p < 0.05$ is considered significant.

3.3 Results and Discussion

To determine if cellulose nanocrystals are appropriate biomaterials that produce no toxic effects, cell viability and cytotoxicity assays were performed. Cell viability was determined by a standard MTT conversion assay. MTT (3-[4,5-dimethyl-2-thiazol]-2,5-diphenyl-2H-tetrazolium bromide) is a tetrazolium salt, which is metabolized within the mitochondria of viable cells. The absorbance of the produced formazan at 570 nm is proportional to the number of living cells in the sample. The viability of an array of brain cells, breast cells, and cancer cells, in percent of cell viability of the control, after exposure to increasing concentrations of cellulose nanocrystals for 48 hours is shown in the left panels of the Figures 9-12. At each concentration of cellulose nanocrystals (10, 25, 50 μg/mL), the cell viability remained within the error margins of the cell viability of the control.

Additionally, an LDH release assay was employed to measure cytotoxicity. Damaged cells release cytoplasmic LDH, which catalyzes a conversion of tetrazolium salt to formazan. The absorbance of the produced formazan at 490 nm is proportional to the number of damaged or dying cells. The cytotoxicity of various cells, in percent of LDH activity of the control, after

exposure to increasing concentrations of cellulose nanocrystals for 48 hours is shown in the right panels of the Figures 9-12. At each concentration, there was no significant cytotoxicity produced.

The cell viability/cytotoxicity results indicate that cellulose nanocrystals are non-toxic to the array of cells tested.

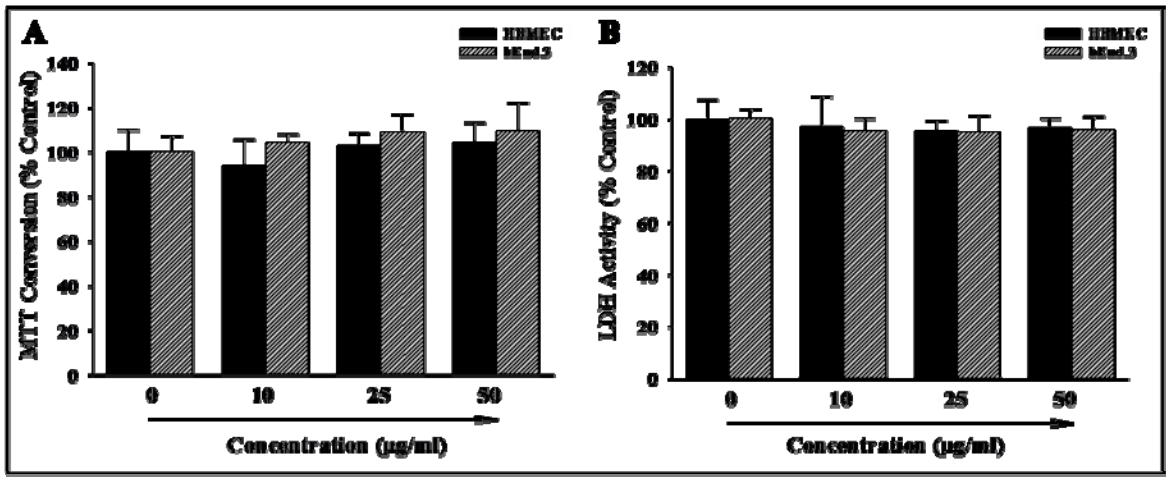

Figure 9: Effects of cellulose nanocrystals on the viability of brain microvascular endothelial cells. MTT (A) and LDH (B) assays with HBMEC and bEnd.3 cells exposed to cellulose nanocrystals at $\leq$ 50 µg/ml for 48 hours revealed no cytotoxic effects. Data are ±SD of 4 determinations.

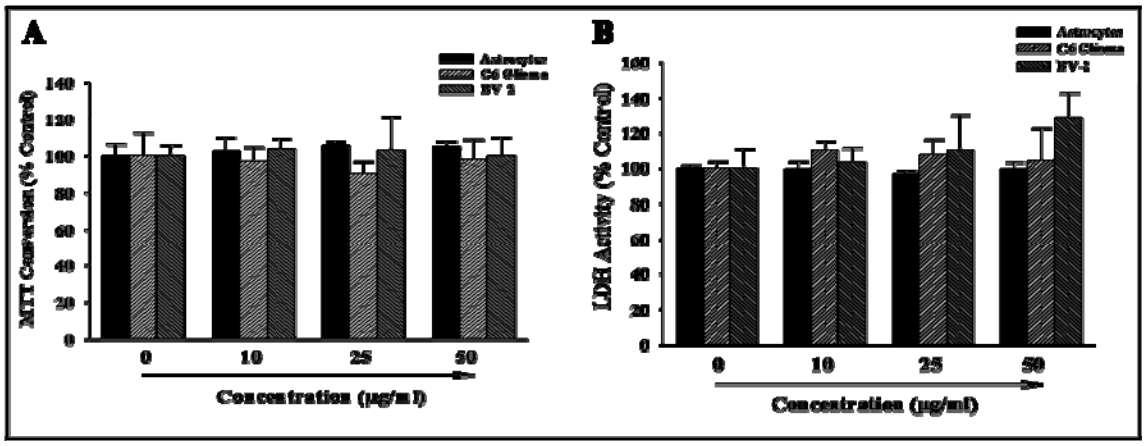

Figure 10: Effects of cellulose nanocrystals on the viability of brain cells. MTT (A) and LDH (B) assays with astrocytes, C6 glioma, and BV-2 cells exposed to cellulose nanocrystals at ≤ 50 µg/ml for 48 hours revealed no cytotoxic effects. Data are ±SD of 4 determinations.

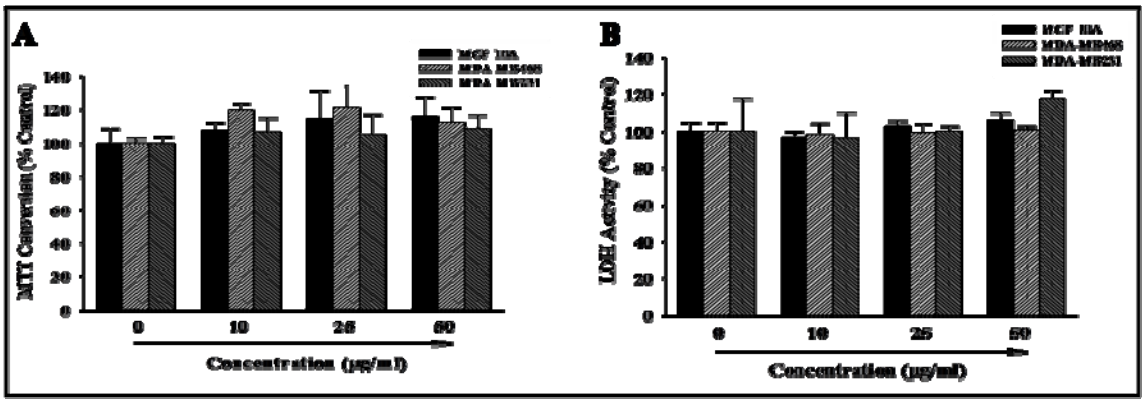

Figure 11: Effects of cellulose nanocrystals on the viability of breast cells. MTT (A) and LDH (B) assays with MCF 10 A, MDA-MB-468, and MDA-MB-231 cells exposed to cellulose nanocrystals at ≤ 50 µg/ml for 48 hours revealed no cytotoxic effects. Data are ±SD of 4 determinations.

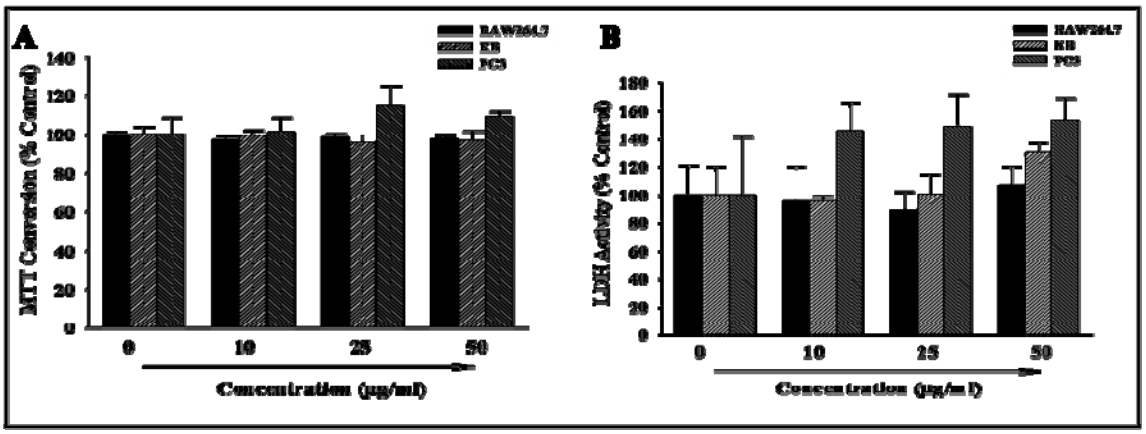

Figure 12: Effects of cellulose nanocrystals on the viability of other cells. MTT (A) and LDH (B) assays with RAW264.7, KB, and PC3 cells exposed to cellulose nanocrystals at ≤ 50 μg/ml for 48 hours revealed no cytotoxic effects. Data are ±SD of 4 determinations.

The second phase of experiments focused on non-specific binding/uptake of cellulose nanocrystals. To conduct the binding/uptake experiments, cellulose nanocrystals were labeled with fluorescein-5'-isothiocyanate (FITC) as described in Materials and Methods. An array of concentrations of FITC-labeled cellulose nanocrystals was prepared by adding a suspension of 0.5 mg/ml FITC-CNC to phosphate-buffered saline in wells of a 96-well plate. The fluorescence intensity of the following concentrations: 0.5, 1, 5, 10, 50, 100, and 500 μg/ml was determined with a fluorescence microplate reader (Molecular Devices SpectraMax M2e) at an excitation and emission wavelength of 485 and 530 nm, respectively. As demonstrated in Figure 13, a significant and dose-dependent increase in fluorescence intensity was detected in FITC-CNC suspension at the concentrations of 1.0 μg/ml and above.

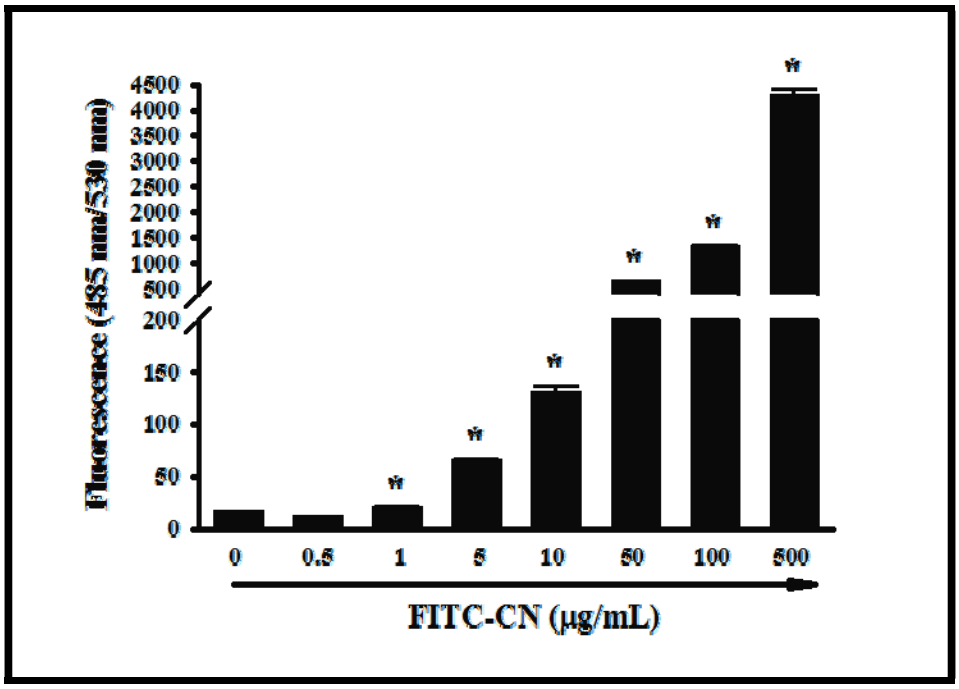

Figure 13: Fluorescence intensity of increasing concentrations of FITC-labeled cellulose nanocrystals as determined by fluorescence microplate reader. Data are ±SD of 4 determinations. *Statistically significant compared with control group ($p < 0.05$).

Non-specific cellular binding/uptake of cellulose nanocrystals was determined by exposing cells to FITC-labeled cellulose nanocrystals for up to 8 hours, after which excess nanocrystals were removed by washing with PBS and the remaining fluorescence was measured. The binding/uptake of 50 µg/ml of FITC-labeled cellulose nanocrystals by brain cells (HBMEC, bend.3, C6 Glioma) for up to 8 hours of exposure is shown in Figure 14A. Additionally, binding/uptake of cellulose nanocrystals was checked in breast cells, such as MCF-10A, MDA-MB468, and MDA-MB231, (Figure 14B) and other immune and cancer cells, such as RAW264.7, KB, and PC3 (Figure 14C). While there is an increase in binding/uptake over time, the actual percentage of cellular binding/uptake is not significant when compared to the control. A low binding/uptake of untargeted nanoparticles is desired in targeted drug delivery

applications as it allows us to control specific binding/uptake through selective targeting mechanisms.

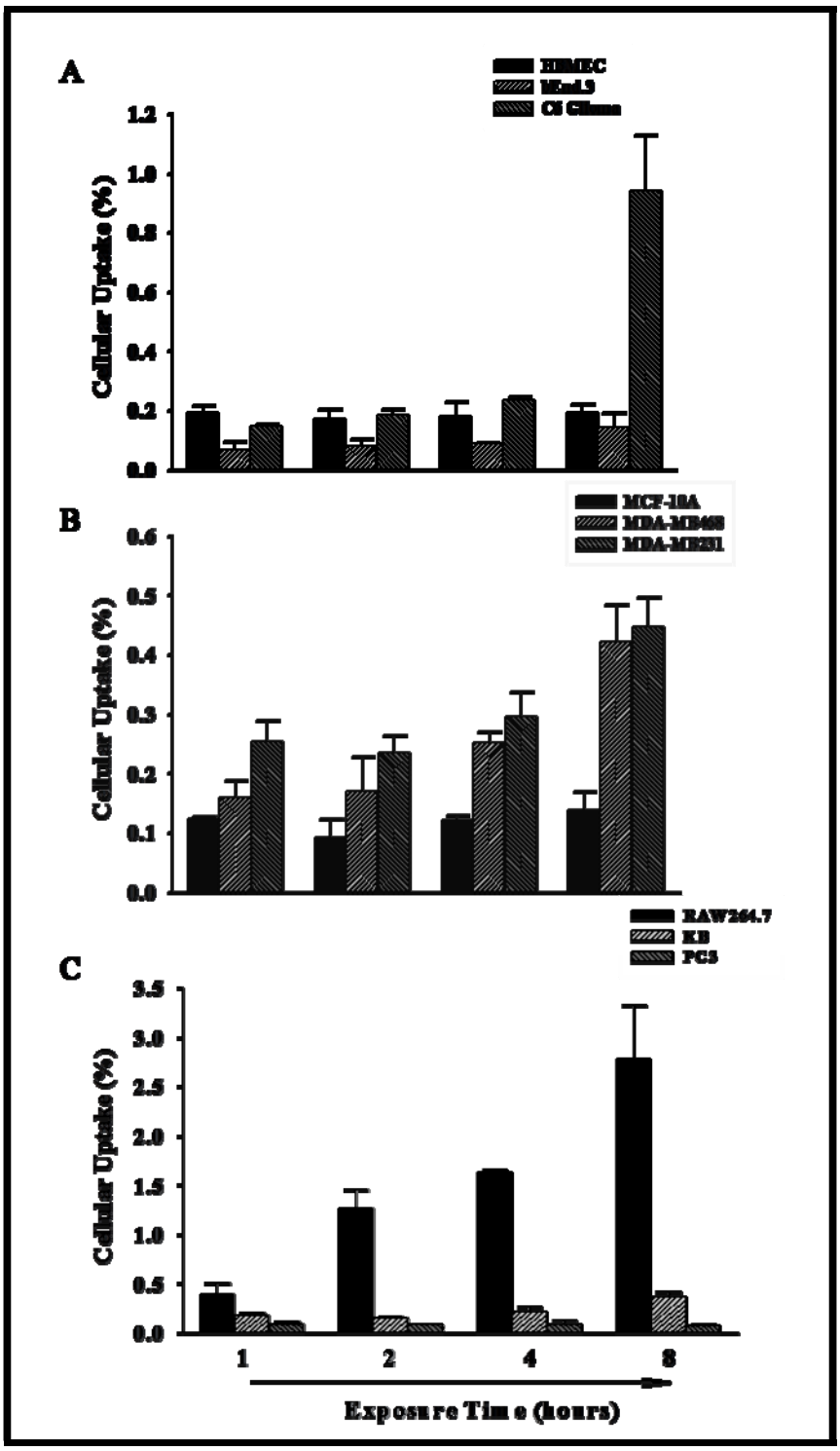

Figure 14: Cellular binding/uptake of FITC-labeled cellulose nanocrystals (FITC-CNC) by brain cells (A), breast cells (B), and other cells (C). Cellular binding/uptake assay by fluorescent microplate reader shows cells treated with 50 μg/ml FITC-CNC for up to 8 hours revealed no significant non-specific binding/uptake. Data are ± SEM of 4 determinations.

We have shown that cellulose nanocrystals are non-toxic to a wide array of cells and that cellular binding/uptake of untargeted cellulose nanocrystals is minimal. The lack of toxicity and untargeted binding/uptake make cellulose nanocrystals promising candidates as carriers in targeted delivery applications. Several factors need to be considered in selecting the targeting molecule. The targeting molecule should be (1) a stable, non-immunogenic structure and (2) highly specific in targeting (Zhang 2008). In consideration of these factors, we have chosen folic acid that has been widely known to specifically target folate receptors. Folate receptors are membrane glycoproteins that are overexpressed in activated inflammatory cells, and most tumor cells (Chandrasekar 2007). These cells can selectively bind and uptake folate conjugates *via* folate receptor-mediated endocytic pathways (Sudimack 2000; Vortherms 2008). Higher affinity binding for the folate receptor is seen when folate is covalently link *via* its γ-carboxyl group to a carrier molecule (Sudimack 2000). Folic acid conjugation to FITC-labeled cellulose nanocrystals was performed in Dr. Roman's laboratory as described in Materials and Methods.

In order to verify the continuous use of our brain inflammation model, the effects of LPS on the expression of folate receptor- α (FR-α) was studied. Expression levels of folate receptor-α was determined by quantitative real-time RT-PCR. As shown in the following figure, mouse macrophage cells (Figure 15A) display a significant increase in FR-α expression after exposure to LPS for 2 hours. Overexpression of FR-α is still displayed at 8 hours, however it decreased slightly. Mouse brain endothelial cells (Figure 15B) show an early response in FR-α expression at 1 hour exposure that begins to decrease at only 2 hours. Mouse microglial cells (Figure 15C) do not show any significant difference in folate receptor expression after being exposed to 100 ng/ml LPS. Expression levels in mouse brain (Figure 15D) display a significant increase in FR-α at 1 hour exposure. These results demonstrate that brain microvascular endothelial cells, macrophages, and mouse brain function as appropriate models for folic acid-targeted nanoparticles.

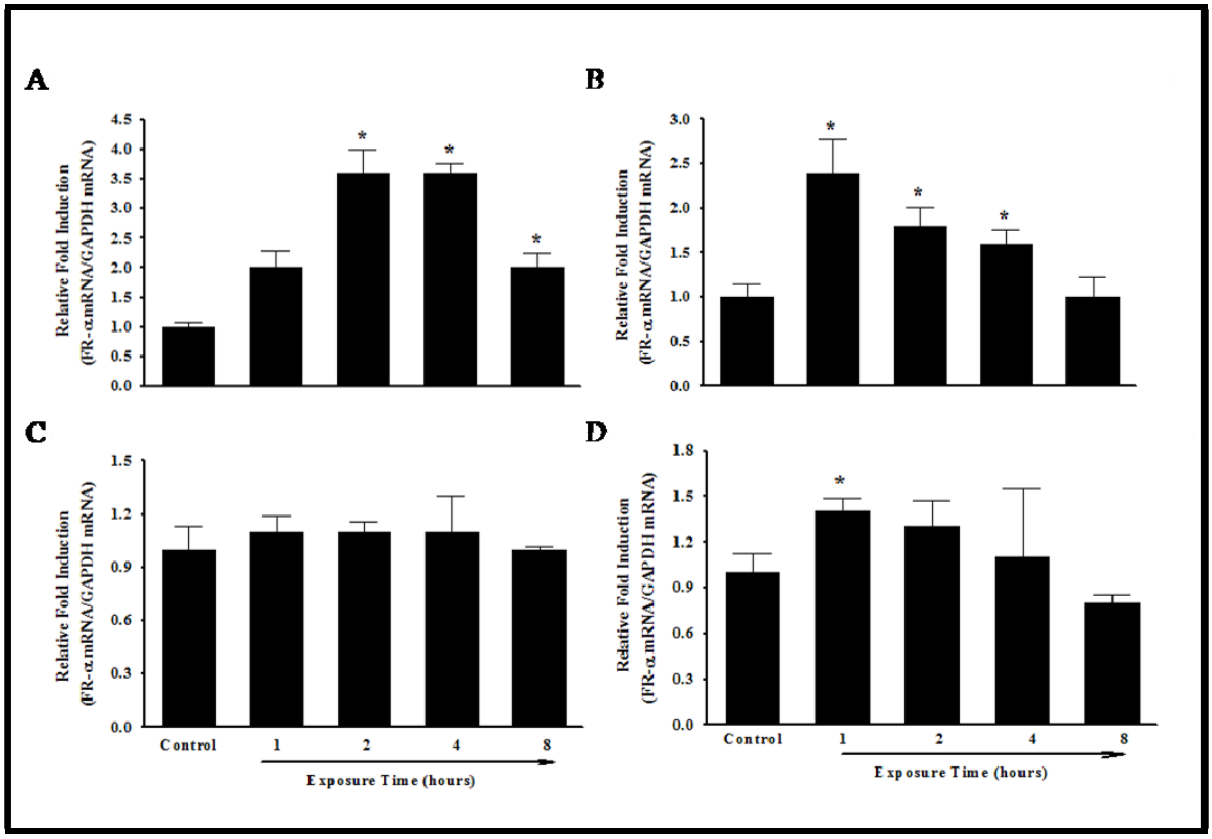

Figure 15: Effects of LPS on the expression of FR-α in mouse macrophage cells (RAW 264.7) (A), mouse brain endothelial cells (bEnd.3) (B), mouse microglial cells (BV-2) (C), and mouse brain (D). Cells (A, B, C) were treated with 100 ng/ml LPS for 1, 2, 4, and 8 hours. Mice (D) were treated with 500 μg/ml LPS for 1, 2, 4, and 8 hours. Expression levels of folate receptor-α were determined by quantitative real-time RT-PCR as described in Materials and Methods. Data are ±SEM of 4 determinations. *Statistically significant compared with control group ($p < 0.05$).

For the initial phase of targeting experiments, we decided to verify our targeting strategy in established folate receptor-positive models and evaluate our inflammation models in the future. The gene expression profile in Figure 16 showed a comparison of FR-α expression in various cancer cells. Normal human breast epithelial cells, MCF-10A, are used as a control for FR-α expression. MDA-MB231 breast carcinoma cells show minimal expression of FR-α. MDA-MB468, breast carcinoma cells, known for their FR-α positive expression show a significant induction fold increase. KB cells, considered as the gold standard for overexpressed FR-α, show a fold increase over 9000. KB and MDA-MB468 will be used for the final targeted binding/uptake experiments.

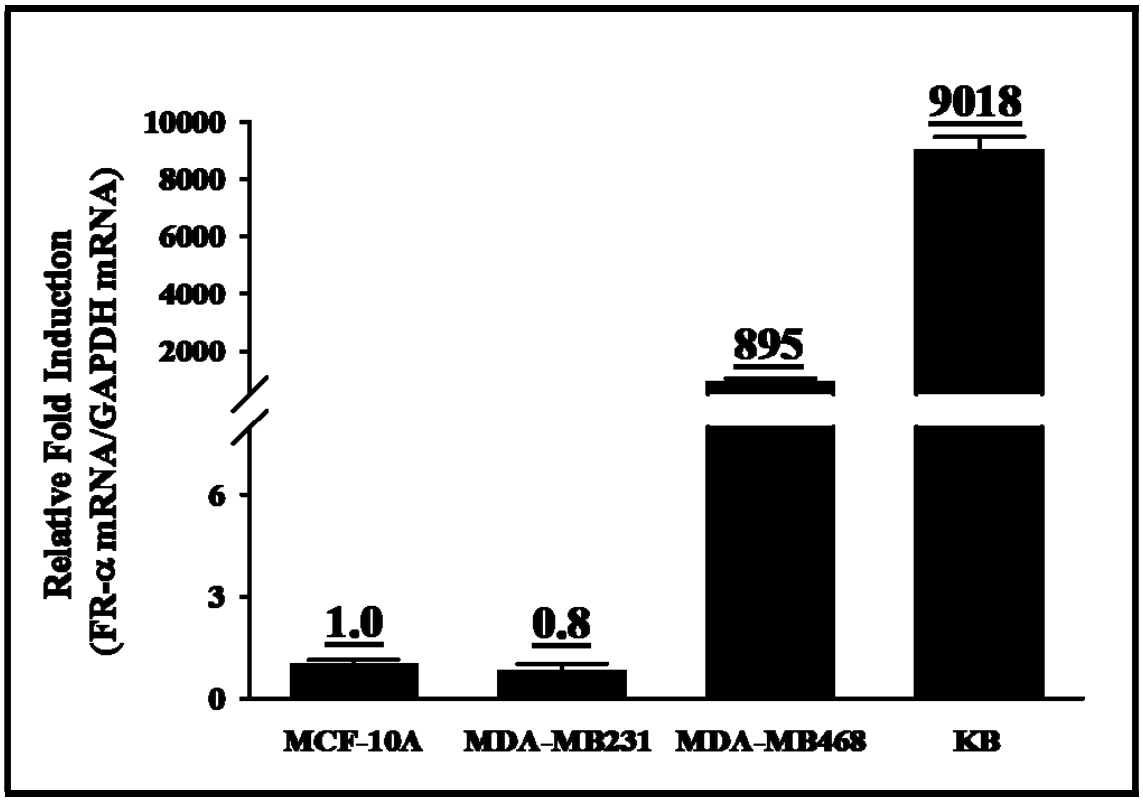

Figure 16: Profile of FR-α expression in cancer cells: MCF-10A, MDA-MB231, MDA-MB468, and KB. Expression levels of folate receptor-α were determined by quantitative real-time RT-PCR as described in Materials and Methods. Data are ±SEM of 4 determinations.

In the final experiment, the fluorescent microscope was employed to study targeted cellular binding/uptake of folic acid-conjugated cellulose nanocrystals. Figures 17 and 18 showed fluorescence microscopic images of the cellular binding/uptake of FITC-CNC and FA-CNC-FITC in FR-positive cancer cells. KB cells were incubated with either CNC conjugated with FITC and FA (FA-CNC-FITC) or CNC conjugated with FITC only (FITC-CNC) for 4 h at 37 °C. The cell membranes were then stained with Concanavalin A AlexaFluor 594 and the slides were examined on a Zeiss AXIO Imager A1m fluorescence microscope. Images were acquired by AxioCam MRc5 Digital Imaging System. Green fluorescence of specifically bound/uptaken FA-CNC-FITC was visible on the red-stained KB cells (Figure 16, D-F) while only weak, non-specific green fluorescence was observed in cells incubated with FITC-CNC (Figure 16, A-C). To further examine the targeting specificity of the FA-conjugated CNC, an additional cellular binding/uptake assay was conducted in KB cells incubated with FA-CNC-FITC in the presence of 1 mM free FA. As illustrated in Figure 16 (G-I), the addition of excess amount of FA caused a marked decrease in the cellular binding/uptake of FA-CNC-FITC. Similar effects were also observed in MDA-MB-468 human breast cancer cells (Figure 17). These results strongly suggest that the FA-conjugated CNC selectively target FR-positive cancer cells, such as KB and MDA-MB-468 cells, *via* FR-mediated mechanism.

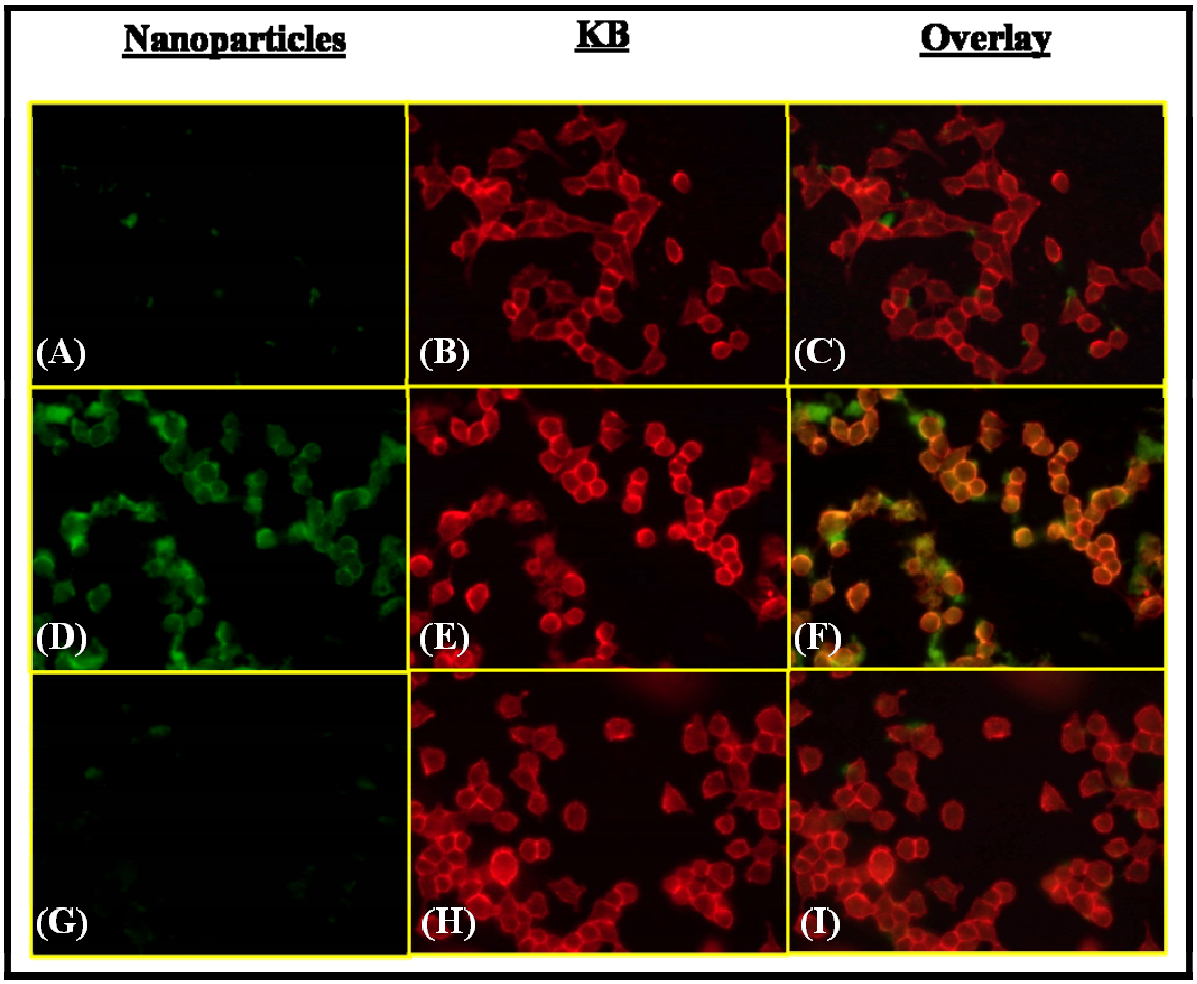

Figure 17: Effect of bioconjugated CNCs on the cellular binding/uptake analyzed by fluorescence microscopy. KB cells were cultured on glass slides for 24 h and incubated with either FITC-CNC (A-C) or FA-CNC-FITC in the absence (D-F) or presence of 1 mM free FA (G-I) for 4 h at 37 °C. (A), (D), and (G) display the green FITC fluorescence of CNCs; (B), (E), and (H) depict the red cell membrane of KB cells stained with Concanavalin A AlexaFluor 594; (C), (F), and (I) overlay of the both green (CNCs) and red (KB cells) fluorescence images.

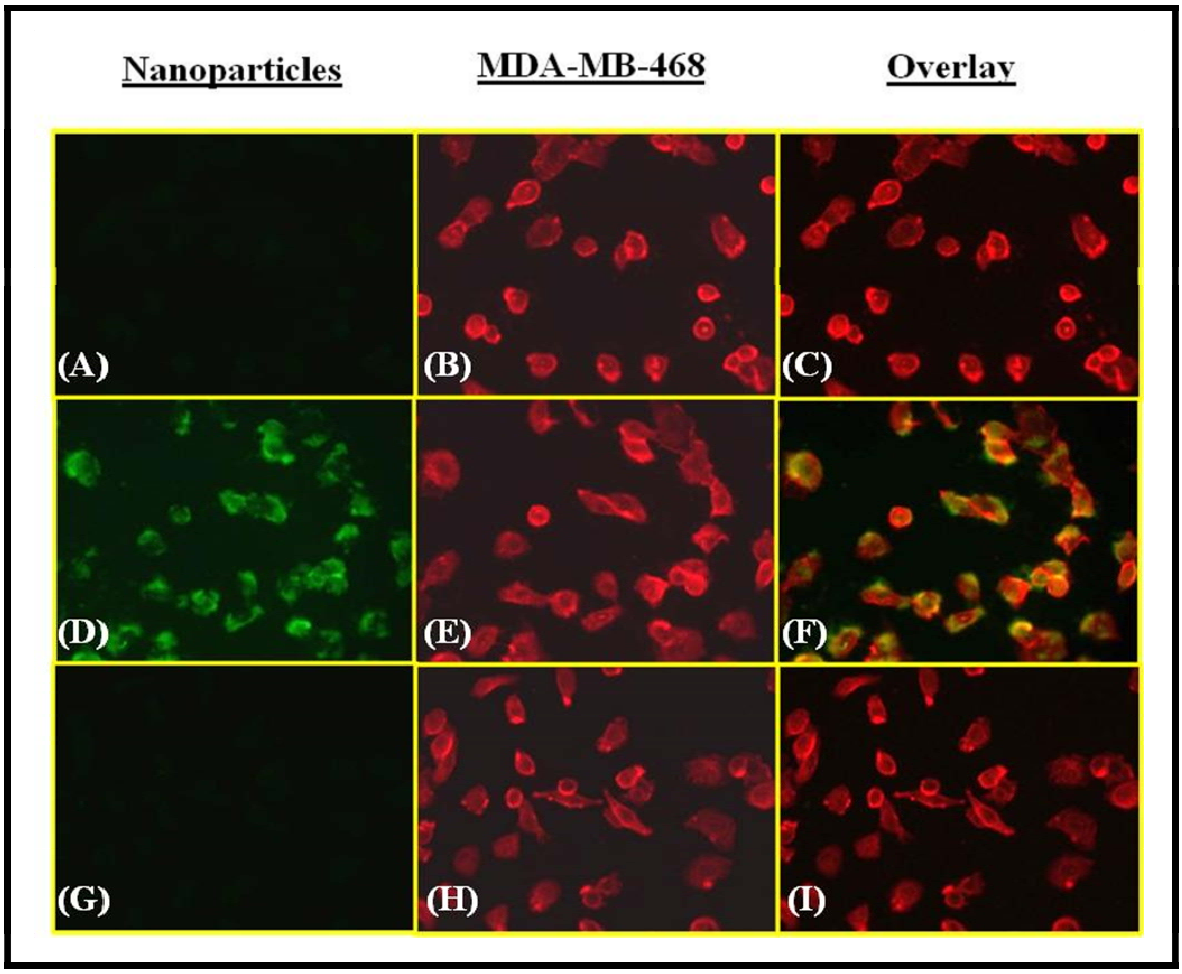

Figure 18: Effect of bioconjugated CNCs on the cellular binding/uptake analyzed by fluorescence microscopy. MDA-MB-468 cells were cultured on glass slides for 24 h and incubated with either FITC-CNC (A-C) or FA-CNC-FITC in the absence (D-F) or presence of 1 mM free FA (G-I) for 4 h at 37 °C. (A), (D), and (G) display the green FITC fluorescence of CNCs; (B), (E), and (H) depict the red cell membrane of MDA-MB-468 cells stained with Concanavalin A AlexaFluor 594; (C), (F), and (I) overlay of the both green (CNCs) and red (MDA-MB-468 cells) fluorescence images.

4. Conclusion

In the present study, we established *in vitro* and *in vivo* brain inflammation models by administering LPS to mouse brain endothelial cells, microglia, macrophage cells, and mouse. The resulting gene expression profile indicated overexpression of pro-inflammatory mediators such as TNF-α, IL-1β, IL-6, MCP-1, E-selectin, and ICAM-1; similar to inflammation profiles generated in neurodegenerative diseases.

For targeted delivery, cellulose nanocrystals were chosen as the biomaterial. Its small size, hydrophilic nature, and ability for surface modification made it a versatile and flexible material to work with. We were able to characterize cellulose nanocrystals as non-toxic with limited binding/uptake in its untargeted state. The lack of toxicity and untargeted binding/uptake make cellulose nanocrystals promising candidates as carriers in targeted delivery applications. In consideration of choosing a targeting molecule that is stable and highly specific, folic acid was chosen as it has been widely known to specifically target folate receptors. Our gene expression profile showed overexpression of folate receptor in inflammatory and cancer cells. Folate targeting of the cellulose nanocrystals was verified in folate receptor-positive cancer cells. The binding/uptake results suggest that the folic acid-conjugated cellulose nanocrystals selectively target cells *via* FR-mediated mechanism.

Further work will include conjugating therapeutic agents on the FA-conjugated cellulose nanocrystals. Anti-inflammatory agents, such as non-steroidal anti-inflammatory drugs (NSAIDS), have been associated with decreased risk of developing neurodegenerative disease and would serve to counteract the progression of neuroinflammation. Antioxidants also make a good candidate target the reactive oxygen species produced by damaged endothelial cells and activated microglia (Rock 2006). In pursuing the cancer model, targeting the folate receptor with anti-cancer drugs have the potential for treatment (Sudimack 2000).

References

Araki J, Wada M, Kuga S, Okano T. (1998). "Flow Properties Of Microcrystalline Cellulose Suspension Prepared By Acid Treatment Of Native Cellulose." Colloids and Surfaces, A: Physicochemical and Engineering Aspects **142**(1): 75–82.

Araki J, Wada M, Kuga S, Okano T. (2000). "Birefringent Glassy Phase Of A Cellulose Microcrystal Suspension." Langmuir **16**(6): 2413–2415.

Beck-Candanedo S, Roman M, Gray DG. (2005). "Effect Of Reaction Conditions On The Properties And Behavior Of Wood Cellulose Nanocrystal Suspensions." Biomacromolecules **6**(2): 1048–1054.

Black SM, Fineman JR. (2006). "Oxidative And Nitrosative Stress In Pediatric Pulmonary Hypertension: Roles Of Endothelin-1 And Nitric Oxide." Vascular Pharmacology **45**: 308-316.

Bone I. (2007). "The Increasing Importance Of Inflammation In Neurological Disease." Current Opinion in Neurology **20**: 331-333.

Carlsson M, Stenman D, Merenyi G, Reitberger T. (2005). "A Comparative Study On The Degradation Of Cotton Linters Induced By Carbonate And Hydroxyl Radicals Generated From Peroxynitrite." Holzforschung **59**(2): 132–142.

Cernak I, Vink R, Zapple DN, Cruz MI, Ahmed F, Chang T, Fricke ST, Faden AI. (2004). "The Pathobiology Of Moderate Diffuse Traumatic Brain Injury As Identified Using A New Experimental Model Of Injury In Rats." Neurobiology of Disease **17**(1): 29-43.

Chandrasekar D, Sistla R, Ahmad FJ, Khar RK, Diwan PV. (2007). "Folate Coupled Poly(Ethyleneglycol) Conjugates Of Anionicpoly(Amidoamine) Dendrimer For

Inflammatory Tissue Specific Drug Delivery." Journal of Biomedical Materials Research **82A**: 92–103.

Chazeau L, Cavaille JY, Canova G, Dendievel R, Boutherin B. (1999). "Viscoelastic Properties Of Plasticized Pvc Reinforced With Cellulose Whiskers." Journal of Applied Polymer Science **71**(11): 1797–1808.

Couvreur P, Vauthier C. (2006). "Nanotechnology: Intelligent Design To Treat Complex Disease." Pharmaceutical Research **23**(7): 1417–1450.

de la Torre JC, Stefano GB. (2000). "Evidence That Alzheimer's Disease Is A Microvascular Disorder: The Role Of Constitutive Nitric Oxide." Brain Research **34**: 119-136.

Dong S, Roman M. (2007). "Fluorescently Labeled Cellulose Nanocrystals For Bioimaging Applications." Journal of the American Chemical Society **129**(45): 13810-13811.

Dong XM, Revol JF, Gray, DG. (1998). "Effect Of Microcrystallite Preparation Conditions On The Formation Of Colloid Crystals Of Cellulose." Cellulose **5**(1): 19–32.

Dumitriu S. (2002). "Polysaccharides As Biomaterials." Polymeric Biomaterials (2nd Edition): 1–61.

Fahrig T, Gerlach I, Horvath E. (2005). "A Synthetic Derivative Of The Natural Product Rocaglaol Is A Potent Inhibitor Of Cytokine-Mediated Signaling And Shows Neuroprotective Activity In Vitro And In Animal Models Of Parkinson's Disease And Traumatic Brain Injury." Molecular Pharmacology **67**(5): 1544-55.

Favier V, Chanzy H, Cavaille JY. (1995). "Polymer Nanocomposites Reinforced by Cellulose Whiskers." Macromolecules **28**(18): 6365–6367.

Fiala M, Zhang L, Gan X, Sherry B, Taub D, Graves MC, Hama S, Way D, Weinand M, Witte M, Lorton D, Kuo YM, Roher AE. (1998). "Amyloid-β Induces Chemokine Secretion And Monocyte Migration Across A Human Blood-Brain Barrier Model." Molecular Medicine **4**: 480-489.

Giri R, Selvaraj S, Miller CA, Hofman F, Yan SD, Stern D, Zlokovic BV, Karla VK. (2002). "Effect Of Endothelial Cell Polarity On β-Amyloid-Induced Migration Of Monocytes Across Normal And AD Endothelium." American Journal of Physiology Cell Physiology **283**: C895-C904.

Godbout JP, Chen J, Abraham J, Richwine AF, Berg BM, Kelley KW, Johnson RW (2005). "Exaggerated Neuroinflammation And Sickness Behavior In Aged Mice After Activation Of The Peripheral Innate Immune System." The FASEB Journal **19**: 1329-1331.

Grunert M, Winter WT. (2002). "Nanocomposites Of Cellulose Acetate Butyrate Reinforced With Cellulose Nanocrystals." Journal of Polymers and the Environment **10**(1/2): 27–30.

Helbert W, Cavaille JY, Dufresne A. (1996). "Thermoplastic Nanocomposites Filled With Wheat Straw Cellulose Whiskers. Part I: Processing And Mechanical Behavior." Polymer Composites **17**(4): 604–611.

Holland AJA, Ford WDA, Bourne AJ. (1997). "Conservative Surgery For Benign Non-Parasitic Splenic Cysts." Pediatric Surgery International **12**(5-6): 353–355.

Kaur C, Singh J, Lim MK, Ng BL, Ling EA. (1997). "Macrophages/Microglia As 'Sensors' Of Injury In The Pineal Gland Of Rats Following A Non-Penetrative Blast." Neuroscience Research **27**(4): 317-322.

Lemarchand C, Gref R, Couvreur P. (2004). "Polysaccharide-Decorated Nanoparticles." European Journal of Pharmaceutics and Biopharmaceutics **58**(2): 327–341.

Li JM, Shah AM. (2004). "Endothelial Cell Superoxide Generation: Regulation And Relevance For Cardiovascular Pathophysiology." American Journal of Physiology – Regulatory, Integrative and Comparative Physiology **287:** R1014-1030.

Liu B, Hong JS. (2003). "Role Of Microglia In Inflammation-Mediated Neurodegenerative Diseases: Mechanisms And Strategies For Therapeutic Intervention." Journal of Pharmacology and Experimental Therapeutics **304**: 1-7.

Livak KJ, Schmittgen TD. (2001). "Analysis Of Relative Gene Expression Data Using Real-Time Quantitative Pcr And The 2(-Delta Delta C(T)) Method." Methods **25**: 402-8.

Marchessault RH, Morehead FF, Walter NM. (1959). "Liquid Crystal Systems From Fibrillar Polysaccharides." Nature **184**(Suppl. No. 9): 632–633.

McGeer PL, McGeer EG. (2004). "Inflammation And The Degenerative Diseases Of Aging." Annals of the New York Academy of Sciences **1035**: 104-116.

McGeer PL, Yasojima K, McGeer EG. (2001). "Inflammation In Parkinson's Disease." Advanced Neurology **86**: 83-89.

Mechoulam R, Spatz M, Shohami E. (2002). "Endocannabinoids And Neuroprotection." Science's STKE: Signal Transduction Knowledge Environment **129**.

Moosmann B, Behl C. (2002). "Antioxidants As Treatment For Neurodegenerative Disorders." Expert Opinion on Investigational Drugs **11**: 1407-1435.

Mosley RL, Benner EJ, Kadiu I, Thomas M, Boska MD, Hasan K, Laurie C, Gendelman E. (2006). "Neuroinflammation, Oxidative Stress And The Pathogenesis Of Parkinson's Disease." Clinical Neuroscience Research **6**(5): 261-281.

Owens DE, Peppas NA. (2006). "Opsonization, Biodistribution, And Pharmacokinetics Of Polymeric Nanoparticles." International Journal of Pharmaceutics **307**(1): 93–102.

Perry VH, Bell MD, Brown HC, Matyszak MK. (1995). "Inflammation In The Nervous System." Current Opinions in Neurobiology **5**: 636-641.

Porath J, Fornstedt N. (1970). "Group Fractionation Of Plasma Proteins On Dipolar Ion-Exchangers." Journal of Chromatography **51**(3): 479–489.

Revol JF, Bradford H, Giasson J, Marchessault RH, Gray DG. (1992). "Helicoidal Self-Ordering Of Cellulose Microfibrils In Aqueous Suspension." International Journal of Biological Macromolecules **14**(3): 170–172.

Revol JF, Godbout L, Dong XM, Gray DG, Chanzy H, Maret G. (1994). "Chiral Nematic Suspensions Of Cellulose Crystallites; Phase Separation And Magnetic Field Orientation." Liquid Crystals **16**(1): 127–134.

Rock RB, Peterson PK. (2006). "Microglia As A Pharmacological Target In Infectious And Inflammatory Diseases Of The Brain." Journal of Neuroimmune Pharmacology **1**: 117-126.

Rosenthal S, Tomlinson I, Adkins EM, Schroeter S, Adams S, Swafford L, McBride J, Wang Y, DeFelice LJ, Blackely RD. (2002). "Targeting Cell Surface Receptors With Ligand-Conjugated Nanocrystals." Journal of the American Chemical Society **124**(17): 4586-94.

Rubin LL, Staddon JM. (1999). "The Cell Biology Of The Blood-Brain Barrier." Annual Review of Neuroscince **22**: 11-28.

Sarkara D, Fisher PB. (2006). "Molecular Mechanisms Of Aging-Associated Inflammation." Cancer Letters **236**: 13-23.

Schulz JB. (2004). "Neuronal Pathology In Parkinson's Disease." Cell and Tissue Research **318**: 135-147.

Schwartz M, Butovsky O, Kipnis J. (2006). "Does Inflammation In An Autoimmune Disease Differ From Inflammation In Neurodegenerative Disease? Possible Implications For Therapy." Journal of Neuroimmune Pharmacology **1**: 4-10.

Sinha TJ, Vasudevan P. (1984). "Blood-Cellulosics Interactions." Biomaterials Medical Devices and Artificial Organs **12**(3-4): 273–287.

Staddon JM, Herrenknecht K, Schulze C, Smales C, Rubin LL. (1995). "Signal Transduction At The Blood-Brain Barrier." Biochemical Society Transactions **23**: 475-479.

Stins MF, Gilles F, Kim KS. (1997). "Selective Expression Of Adhesion Molecules On Human Brain Microvascular Endothelial Cells." Journal of Neuroimmunology **76**: 81-90.

Sudimack J, Lee RJ. (2000). "Targeted Drug Delivery Via The Folate Receptor." Advanced Drug Delivery Reviews **41** 147-162.

Suo Z, Tan J, Placzek A, Crawford F, Fang C, Mullan M. (1998). "Alzheimer's β-Amyloid Peptides Induce Inflammatory Cascade In Human Vascular Cells: The Role Of Cytokines And CD40." Brain Research **807**: 110-117.

Swoboda G, Hasselbach W. (1985). "Reaction Of Fluorescein Isothiocyanate With Thiol And Amino-Groups Of Sarcoplasmic Atpase." Zeitschrift fuer Naturforschung, C: Biosciences **40**(11-12): 863–875.

Taniyama Y, Griendling KK. (2003). "Reactive Oxygen Species In The Vasculature: Molecular And Cellular Mechanisms." Hypertension **42:** 1075-1081.

Toborek M, Lee YW, Flora G, Pu H, Andras IE, Wylegala E, Hennig B, Nath A. (2005). "Mechanisms Of The Blood-Brain Barrier Disruption In HIV-1 Infection." Cell and Molecular Neurobiology **25**: 181-199.

Valko M, Leibfritz D, Moncol J, Cronin MT, Mazur M, Telser J. (2007). "Free Radicals And Antioxidants In Normal Physiological Functions And Human Disease." The International Journal of Biochemistry & Cell Biology **39**(1): 44-84.

Vestweber D. (1992). "Selectins: Cell Surface Lectins Which Mediate The Binding Of Leukocytes To Endothelial Cells." Seminars in Cell Biology **3**(3): 211-20.

Vestweber D. (2002). "Regulation Of Endothelial Cell Contacts During Leukocyte Extravasation." Current Opinion in Cell Biology **14**(5): 587-93.

Vortherms AR, Doyle RP, Gao D, Debrah O, Sinko PJ. (2008). "Synthesis, Characterization, And In Vitro Assay Of Folic Acid Conjugates Of 3'-Azido-3'-Deoxythymidine (AZT): Toward Targeted AZT Based Anticancer Therapeutics." Nucleosides, Nucleotides and Nucleic Acids **27**(2): 173 - 185.

Yoo HS, Park TG. (2001). "Biodegradable Polymeric Micelles Composed Of Doxorubicin Conjugated PLGA–PEG Block Copolymer." Journal of Controlled Release **70** 63– 70.

Yoo HS, Park TG (2004). "Folate-Receptor-Targeted Delivery Of Doxorubicin Nano-Aggregates Stabilized By Doxorubicin–PEG–Folate Conjugate." Journal of Controlled Release **100**: 247–256.

Zhang Y, Kohler N, Zhang M. (2001). "Intracellular Uptake Of Poly(Ethylene Glycol) And Folic Acid Modified Magnetite Nanoparticles." Materials Research Society Symposium Proceedings **676** Y9.8.1 - Y9.8.5.

Zhang J, Rana S, Srivastava RS, Misra RD. (2008). "On The Chemical Synthesis And Drug Delivery Response Of Folate Receptor-Activated, Polyethylene Glycol-Functionalized Magnetite Nanoparticles." Acta Biomaterialia **4**: 40–48.

Zhou XY, Wu P, Zhang L, Xiong W, Li YS, Feng YM, Ye DY. (2007). "Effects Of Lipoxin A4 On Lipopolysaccharide Induced Proliferation And Reactive Oxygen Species Production In RAW264.7 Macrophages Through Modulation Of G-CSF Secretion." Inflammation Research **56**: 324-333.

Achievements

Awards

1. Travel Award, Graduate Student Association Travel Fund Program, 2007
2. Poster Award, Graduate Research Symposium, 2007

Journal Publications

1. Lee YW, Hirani AA, Kyprianou N, Toborek M. Human immunodeficiency virus-1 Tat protein up-regulates interleukin-6 and interleukin-8 expression in human breast cancer cells. Inflammation Research. 2005;54:380-389.
2. Lee YW, Hirani A. A. Role of interleukin-4 in atherosclerosis. Archives of Pharmacal Research. 2006;29:1-15.
3. Roman M, Dong S, Hirani A, Lee YW. Cellulose nanocrystals for drug delivery. In: Polysaccharide Materials: Performance by Design, Edgar KJ, Heinze T, Buchanan C. Eds., ACS Symposium Series, American Chemical Society, Washington, DC. 2009; In press.

Abstract Publications

1. Hirani AA, Kang S, Ehrich M, Lee YW. Vascular endothelial injury by chlorpyrifos: Relationship to brain metastasis. Proceedings of American Cancer Society 24th Annual Seminar of Cancer Researchers in Virginia. 2005: Absract#29.
2. Lee YW, Hirani AA, Ehrich M. Chlorpyrifos induces BBB disruption through up-regulation of pro-inflammatory mediators in brain microvascular endothelial cells. Toxicologist. 2006;90:1469.
3. Hirani AA, Zhao W, Robbins ME, Sonntag WE, Lee YW. Molecular mechanisms of radiation-induced brain injury. FASEB Journal. 2006;20:A378.

4. Lee YW, Hirani AA. Genistein attenuates pro-inflammatory pathways in human brain microvascular endothelial cells. FASEB Journal. 2006;20:A597.
5. Lee YW, Hirani AA. Signaling mechanisms of interleukin-4-induced pro-inflammatory pathways in human vascular endothelial cells. FASEB Journal. 2006;20:A1186.
6. Layman JM, Hirani AA, McKee MG, Britt PF, Pickel JM, Lee YW, Long TE. Randomly branched poly(2-dimethylaminoethylmethacrylate) polyelectrolytes as gene transfection agents. Polymer Preprints 2006;47:39.
7. Kang S, Lee WH, Hirani AA, Vlachos PP, Lee YW. A multilayer design of parallel-plate flow chamber for studies of endothelial cell response to fluid shear stress. FASEB Journal. 2007;21:587.2.
8. Lee WH, Kang S, Hirani AA, Vlachos PP, Lee YW. Biomedical research applications of a novel double-layer parallel-plate flow chamber. FASEB Journal. 2007;21:899.4.
9. Hirani AA, Lee WH, Kang S, Lee YW. Endothelial cell targeting of lipopolysaccharide-induced brain inflammation. FASEB Journal. 2007;21:749.8.
10. Hirani AA, Lee WH, Kang S, Ehrich M, Lee YW. Chlorpyrifos induces pro-inflammatory environment in discrete regions of mouse brain. FASEB Journal. 2007;21:785.4.
11. Lee WH, Kang S, Hirani AA, Lee YW. A novel double-layer parallel-plate flow chamber. Proceedings of the 33rd Northeast Bioengineering Conference. 2007;53.
12. Meldrum B, Balbuena P, Fuhrman K, Wise B, Hirani AA, Lee YW, Ehrich M. Transfer of lead acetate through an in vitro blood-brain barrier system. Toxicologist. 2007;96:707.
13. Dong S, Hirani AA, Lee YW, Roman M. Cellulose nanocrystals as targeted drug delivery systems. Proceedings of the 233rd ACS National Meeting. 2007.
14. Layman JM, Hirani AA, Hunley MT, Lee YW, Lepene B, Thatcher CD, Long TE. Macromolecules with tailored non-covalent interactions for biomedical applications. Proceedings of the 233rd ACS National Meeting. 2007.
15. Lepene BS, Williams SR, Long TE, Hirani AA, Lee YW, Thatcher CD. Folate targeted glutathione antioxidant delivery systems and their impact on intracellular oxidative status. Proceedings of the 234th ACS National Meeting. 2007.
16. Dong S, Hirani AA, Lee YW, Roman M. Cellulose nanocrystals as for targeted drug delivery applications. Proceedings of the 235rd ACS National Meeting. 2008.

17. Lee YW, Lee WH, Hirani AA. Oxidative mechanisms of interleukin-4 (IL-4)-induced IL-6 expression in human aortic endothelial cells. Program Book of the HEART UK 22nd Annual Conference. 2008.
18. Choi DC, Navarro F, Hirani A, Lee YW, Roman M. Ink-jet printed cellulose nanocrystal substrates for cell micropatterning. Proceedings of the Adhesion Society Annual Meeting. 2009.
19. Choi DC, Navarro F, Hirani A, Lee YW, Roman M. Ink-jet printed cellulose nanocrystal substrates for cell micropatterning. Proceedings of the 237rd ACS National Meeting. 2009.
20. Illing D, Jiang F, Hirani A, Lee YW, Roman M. Enzymatic degradation of cellulose nanocrystals under physiological conditions. Proceedings of the 237rd ACS National Meeting. 2009.

Presentations

1. Hirani AA, Kang S, Ehrich M, Lee YW. 2005. Vascular endothelial injury by chlorpyrifos: Relationship to brain metastasis. *American Cancer Society 24th Annual Seminar of Cancer Researchers in Virginia, University of Virginia Health System, Charlottesville, VA*
2. Lee YW, Hirani AA, Ehrich M. 2006. Chlorpyrifos induces BBB disruption through up-regulation of pro-inflammatory mediators in brain microvascular endothelial cells. *Society of Toxicology 45th Annual Meeting and ToxExpo, San Diego, CA*
3. Hirani AA, Kang S, Ehrich M, Lee YW. 2006. Nanocrystal immunotargeting of chlorpyrifos-mediated vascular inflammation. *MILES-IGERT 2006 Industrial Tour.*
4. Hirani AA, Zhao W, Robbins ME, Sonntag WE, Lee YW. 2006. Molecular mechanisms of radiation-induced brain injury. *Experimental Biology 2006 Annual Meeting, San Francisco, CA*
5. Lee YW, Hirani AA. 2006. Genistein attenuates pro-inflammatory pathways in human brain microvascular endothelial cells. *Experimental Biology 2006 Annual Meeting, San Francisco, CA*
6. Lee YW, Hirani AA. 2006. Signaling mechanisms of interleukin-4-induced pro-

inflammatory pathways in human vascular endothelial cells. *Experimental Biology 2006 Annual Meeting, San Francisco, CA*

7. Layman JM, Hirani AA, McKee MG, Britt PF, Pickel JM, Lee YW, Long TE. 2006. Randomly branched poly(2-dimethylaminoethylmethacrylate) polyelectrolytes as gene transfection agents. *Excellence in Graduate Polymer Research Symposium, American Chemical Society National Meeting, Atlanta, GA*
8. Lee WH, Kang S, Hirani AA, Lee YW. 2007. A novel double-layer parallel-plate flow chamber. *Northeast BMES 2007 Annual Meeting, Stony Brook, NY*
9. Meldrum B, Balbuena P, Fuhrman K, Wise B, Lee YW, Hirani A, Ehrich M. 2007. Transfer of lead acetate through an *in vitro* blood-brain barrier. *Society of Toxicology 46th Annual Meeting and ToxExpo, Charlotte, NC*
10. Dong S, Hirani AA, Lee YW, Roman M. 2007. Cellulose nanocrystals as targeted drug delivery systems. *The 233rd American Chemical Society National Meeting, Chicago, IL*
11. Layman JM, Hirani AA, Hunley MT, Lee YW, Lepene B, Thatcher CD, Long TE. 2007. Macromolecules with tailored non-covalent interactions for biomedical applications. *The 233rd American Chemical Society National Meeting, Chicago, IL*
12. Hirani AA, Dong S, Roman M, Lee YW. 2007. Biomedical Applications of Cellulose Nanocrystals: Targeting Brain Endothelial Cells. *Virginia Tech GSA Research Symposium, Blacksburg, VA*
13. Kang S, Lee WH, Hirani AA, Vlachos PP, Lee YW. 2007. A multilayer design of parallel-plate flow chamber for studies of endothelial cell response to fluid shear stress. *Experimental Biology 2007 Annual Meeting, Washington, DC*
14. Lee WH, Kang S, Hirani AA, Vlachos PP, Lee YW. 2007. Biomedical research applications of a novel double-layer parallel-plate flow chamber. *Experimental Biology 2007 Annual Meeting, Washington, DC*
15. Hirani AA, Lee WH, Kang S, Lee YW. 2007. Endothelial cell targeting of lipopolysaccharide-induced brain inflammation. *Experimental Biology 2007 Annual Meeting, Washington, DC*
16. Hirani AA, Lee WH, Kang S, Ehrich M, Lee YW. 2007. Chlorpyrifos induces pro-inflammatory environment in discrete regions of mouse brain. *Experimental Biology 2007 Annual Meeting, Washington, DC*

17. Lepene BS, Williams SR, Long TE, Hirani AA, Lee YW, Thatcher CD. 2007. Folate targeted glutathione antioxidant delivery systems and their impact on intracellular oxidative status. *The 234th American Chemical Society National Meeting, Boston, MA*
18. Dong S, Hirani AA, Lee YW, Roman M. 2008. Cellulose nanocrystals for targeted drug delivery applications. *The 235rd ACS National Meeting, New Orleans, LA*
19. Lee YW, Lee WH, Hirani AA. 2008. Oxidative mechanisms of interleukin-4 (IL-4)-induced IL-6 expression in human aortic endothelial cells. *HEART UK 22nd Annual Conference 2008, Hatfield, United Kingdom*
20. Choi DC, Navarro F, Hirani A, Lee YW, Roman M. 2009. Ink-jet printed cellulose nanocrystal substrates for cell micropatterning. *Adhesion Society Annual Meeting & Expo, Savannah, GA*
21. Choi DC, Navarro F, Hirani A, Lee YW, Roman M. 2009. Ink-jet printed cellulose nanocrystal substrates for cell micropatterning. *The 237th American Chemical Society National Meeting, Salt Lake City, UT*
22. Illing D, Jiang F, Hirani A, Lee YW, Roman M. 2009. Enzymatic degradation of cellulose nanocrystals under physiological conditions. *The 237th American Chemical Society National Meeting, Salt Lake City, UT*